General Disclaimer

One or more of the Following Statements may affect this Document

- This document has been reproduced from the best copy furnished by the organizational source. It is being released in the interest of making available as much information as possible.

- This document may contain data, which exceeds the sheet parameters. It was furnished in this condition by the organizational source and is the best copy available.

- This document may contain tone-on-tone or color graphs, charts and/or pictures, which have been reproduced in black and white.

- This document is paginated as submitted by the original source.

- Portions of this document are not fully legible due to the historical nature of some of the material. However, it is the best reproduction available from the original submission.

Produced by the NASA Center for Aerospace Information (CASI)

NUS-277

MASTEP

COMPARISON OF NUCLEAR AND EXPLOSIVE DESTRUCT CONCEPTS FOR NUCLEAR ROCKET ENGINES

For

Space Nuclear Propulsion Office
AEC - NASA

Contract SNPC-6

NUS CORPORATION

By

Albert W. De Agazio
Technical Associate

May 1966

Environmental Safeguards Division
1730 M Street, N. W.
Washington, D.C. 20036

COMPARISON OF NUCLEAR AND EXPLOSIVE DESTRUCT
CONCEPTS FOR NUCLEAR ROCKET ENGINES

For

Space Nuclear Propulsion Office
Atomic Energy Commission
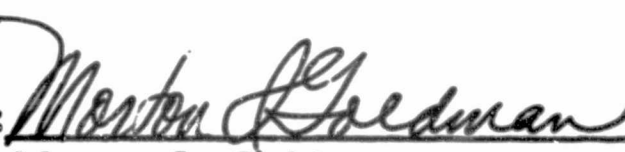National Aeronautics and Space Administration

Contract SNPC-6

By

Albert W. De Agazio

May 1966

Approved: *Morton I. Goldman*
Morton I. Goldman
Vice President
Environmental Safeguards Division

TABLE OF CONTENTS

LIST OF TABLES

LIST OF FIGURES

I. INTRODUCTION

In the event of malfunction which would allow the premature re-entry of the nuclear rocket engine, it may be desirable to fragment the reactor core to minimize the radiation effects to the potentially affected population. The most effective disposal method would be to completely vaporize the core material to obtain as much atmospheric dispersion as possible. However, complete vaporization of the core does not appear to be achievable and, consequently, systems have been investigated which will vaporize a small portion of the core and fragment the remainder allowing these fragments to be dispersed as widely as possible.

For certain circumstances, it might be desirable to allow the reactor to re-enter intact (e.g., if it is certain impact would be in deep ocean or in unpopulated regions). Such disposal might even be as desirable as fragmenting the reactor when impact is in lightly populated areas. The selection of intact or dispersed re-entry, however, is not the object of this report but is treated elsewhere.[1,2]

One means of disposal of a spent nuclear engine to prevent return to earth of large radioactive fragments is to fragment the engine core by explosive means. The small fragment size plus the subsequent dispersal effects of re-entry would be relied upon primarily to reduce the possible dose to a low value. Additionally, the dispersion of the particles throughout the atmosphere reduces the probability of exposure of any individual to a significant number of radioactive fragments.

Dose and exposure probability models have been developed elsewhere;[3,4] however, a number of input parameters required to provide realistic results from these models need better definition.

Fragmentation of the nuclear engine can be accomplished by either of two methods. The nuclear stage can be equipped with the means to fire chemical high explosives into the core and simultaneously detonate these charges at the proper moment to accomplish the desired fragmentation. Alternately, the nuclear engine can be designed such that sufficient reactivity can be inserted to cause a rapid energy release within the fuel itself to accomplish fragmentation.

Although the end result may be similar the mechanism of fragmentation produced by these two methods differs greatly. The chemical high explosive method causes fragmentation initially by the generation of a shock wave. As the first fragments produced accelerate and move away from the charge location, crushing and grinding occurs, causing further particle attrition, in addition to the shock wave damage.

The nuclear destruct method, on the other hand, deposits energy within the fuel material in the matrix, causing high temperatures and pressures which produces the fragmentation.

It is to be expected that the fragmentation produced by such differing mechanisms could differ widely. It is the definition of these differences in fragmentation characteristics and the consequent biological inter-actions that is the objective of this report.

II. CHARACTERISTICS OF ENGINE DESTRUCT SYSTEMS

A. CHEMICAL HIGH EXPLOSIVE DESTRUCT

The details of the high explosive destruct system configuration has been the subject of another report [5] and, consequently, will only be briefly described here.

Basically the presently conceived system consists of implanting four high explosive charges which are contained in modified 105 mm artillery shells, each equipped with its own externally triggered detonator. Before use, the shells are contained in launcher tubes attached to the upper engine support structure. When the destruct system is energized, the explosive shells are fired from the launcher tubes, penetrate the shields and engine pressure vessel dome, and enter the reactor core. When the shells have travelled the proper distance into the core, the four high explosive charges are simultaneously detonated.

A number of tests have been conducted to determine the degree of fragmentation and other characteristics produced by chemical high explosives. These tests include both scale model bench tests and full scale field tests. All the tests, however, with the exception of one, used statically emplaced explosive charges to fragment the core model. The one test that did not use a statically emplaced charge was an early test to demonstrate the feasibility of firing an explosive charge from a launcher (the test used a 105 mm howitzer) and detonating the charge after the shell had travelled a specified distance into the core.

This report will consider only those tests which used simulated ROVER fuel material and consequently is limited to the following tests:

    a.   APG-3 full scale test
    b.   Scale model test at LASL--1/9 scale
    c.   Fuel fragmentation tests at LASL--1 inch samples.

The APG-2 test conducted at Aberdeen Proving Grounds did not mockup the entire core model with simulated fuel. The size distribution, however, from this test is included even though only four size classes were used.

A number of parameters from these tests must be examined to determine the characteristics of high explosive destruct systems. These parameters are:

    a.   the particle size distribution which indicates the degree of fragmentation of the reactor core and the effect of temperature upon fragmentation. Both mass and number distributions as a function of size are required.

    b.   the distribution of fragments about the origin to indicate non-uniform dispersion

    c.   the fission product distribution as a function of particle size required to determine the dose delivered per particle

    d.   fission product solubility to determine the degree of internal organ exposure that will occur.

1.   Size Distribution

Figure 1 shows the size distributions produced in the APG-2,[6] APG-3[7] and 1/9 scale LASL[8] Test. One-ninth scale test results are shown by two curves shown on Figure 1; one curve is for a 1864 g sample while the other is for a 28.9 g sample. These two curves differ by a maximum of approximately 10 to 12 percent by weight.

The mass median diameter of the 1864 g sample of one-ninth scale model debris is 1260 microns and for the smaller 28.9 g sample is 1860 microns. The limited data from the APG-2 test lie between the size distributions of the two one-ninth scale samples.

The mass median diameter from the APG-3 test is 3160 microns indicating that a much coarser fragmentation of the core occurred.

Unlike the one-ninth scale test which used a single axial charge, the APG-3 test simulated the placement of the explosive in four charges placed symetrically about the axis midway between center and the edge of the graphite core. Thus, it is not surprising that

Figure 1.

SIZE DISTRIBUTION FROM APG-2, APG 3 AND LASL ONE-NINTH SCALE
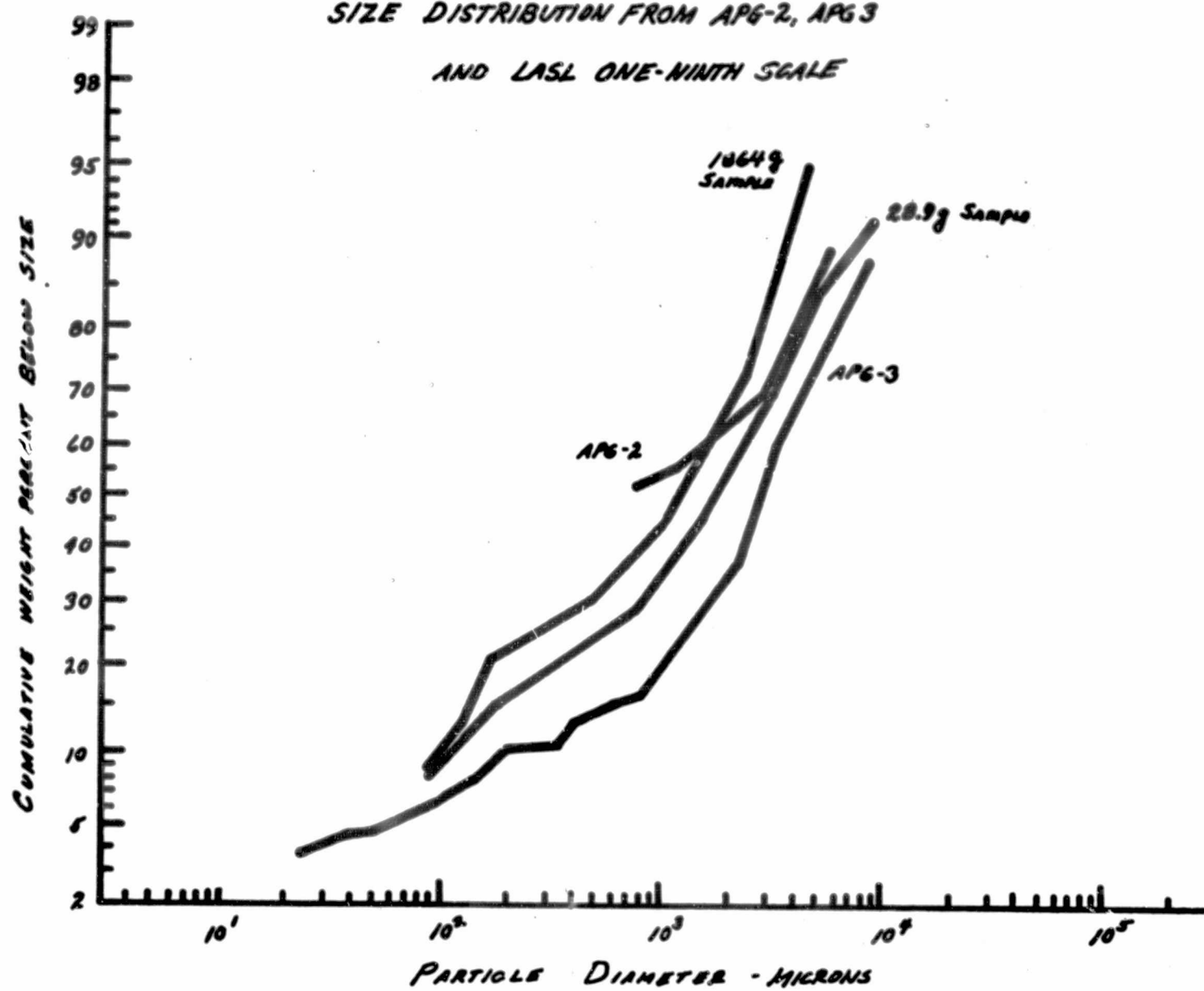
the size distribution for the APG-3 results differs from the one-ninth scale test. It is surprising, however, that the shape of the distribution curves are similar. This leads one to speculate that the differences are due more to the inherent difficulties of scaling such experiments than in different fragmentation characteristics due to the geometry of the explosive charges.

The APG-3 test was the best instrumented and most analyzed test yet conducted. Consequently, for the purposes of this report the APG-3 test results for size distribution will be taken as representative of the size distribution that can be obtained from a ROVER reactor. Figure 2 shows the number of particles and the average weight of the particles as a functing of size for a high explosive destruct.

None of the scale model or full size tests conducted have considered the effect of temperature. Thus, these tests do not define the size distribution that would be obtained from the explosive destruct of a reactor which has been in a high temperature environment during operation and may be at elevated temperatures at the time the destruct system is activated.

Los Alamos Scientific Laboratory* has conducted a series of experiments with one-inch long pieces of fuel material. This fuel material was subjected to various pretreatment temperatures to simulate reactor operation and was held at various temperatures at the time a small charge of explosive was detonated. Figures 3 through 6 show the size distributions obtained for the various samples. Table I summarizes the pretreatment and temperature at the time of fragmentation.

---

* This data was made available through the courtesy of Mr. H. Schulte of the Industrial Hygiene Group of Los Alamos Scientific Laboratory.

FIGURE 2

NUMBER OF PARTICLES AND
PARTICLE WEIGHT FROM
APG-3 TEST

NUMBER

WEIGHT

NUMBER OF PARTICLES LARGER THAN INDICATED SIZE

AVERAGE PARTICLE WEIGHT, GRAMS

PARTICLE DIAMETER, MICRONS
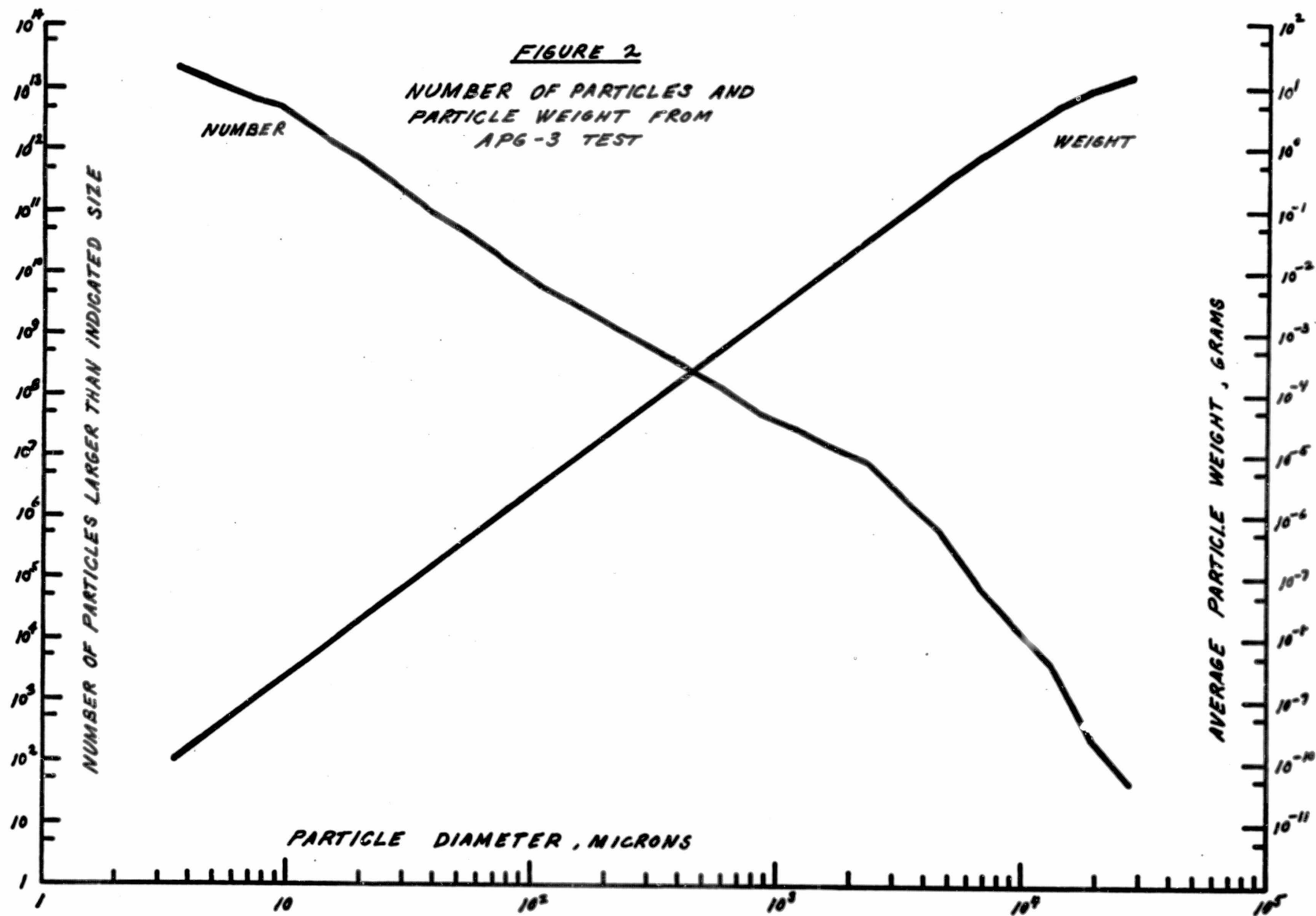
TABLE I

SUMMARY OF PREHEAT AND FRAGMENTATION TEMPERATURES

Sample	Fuel Type	Preheat Temperature and Time		Temperature at Fragmentation
A	Unbeaded	No Preheat		Ambient
B	Beaded	No Preheat		Ambient
C	"	No Preheat		Ambient
D	"	No Preheat		Ambient
E	Unbeaded	2200°C	30 Minutes	Ambient
F	Beaded	2200°C	30 Minutes	Ambient
G	"	2500°C	180 Minutes	Ambient
H	Unbeaded	No Preheat		2500° C
I	Beaded	No Preheat		2500° C
J	"	No Preheat		2500° C
K	"	No Preheat		2670° C
L	"	2200°C	30 Minutes	2500° C
M	"	2500°C	180 Minutes	2500° C
N	"	2500°C	180 Minutes	2655° C
O	"	2500°C	180 Minutes	2765° C
P	Unbeaded	2200°C	30 Minutes	2500° C

FIGURE 3

EFFECT OF TEMPERATURE
UPON FRAGMENTATION

CURVE	PREHEAT	FRAGMENTATION
A	NONE	AMBIENT
B	NONE	AMBIENT
C	NONE	AMBIENT
D	NONE	AMBIENT

PARTICLE DIAMETER, MICRONS

CUMULATIVE FRACTION BY WEIGHT BELOW INDICATED SIZE
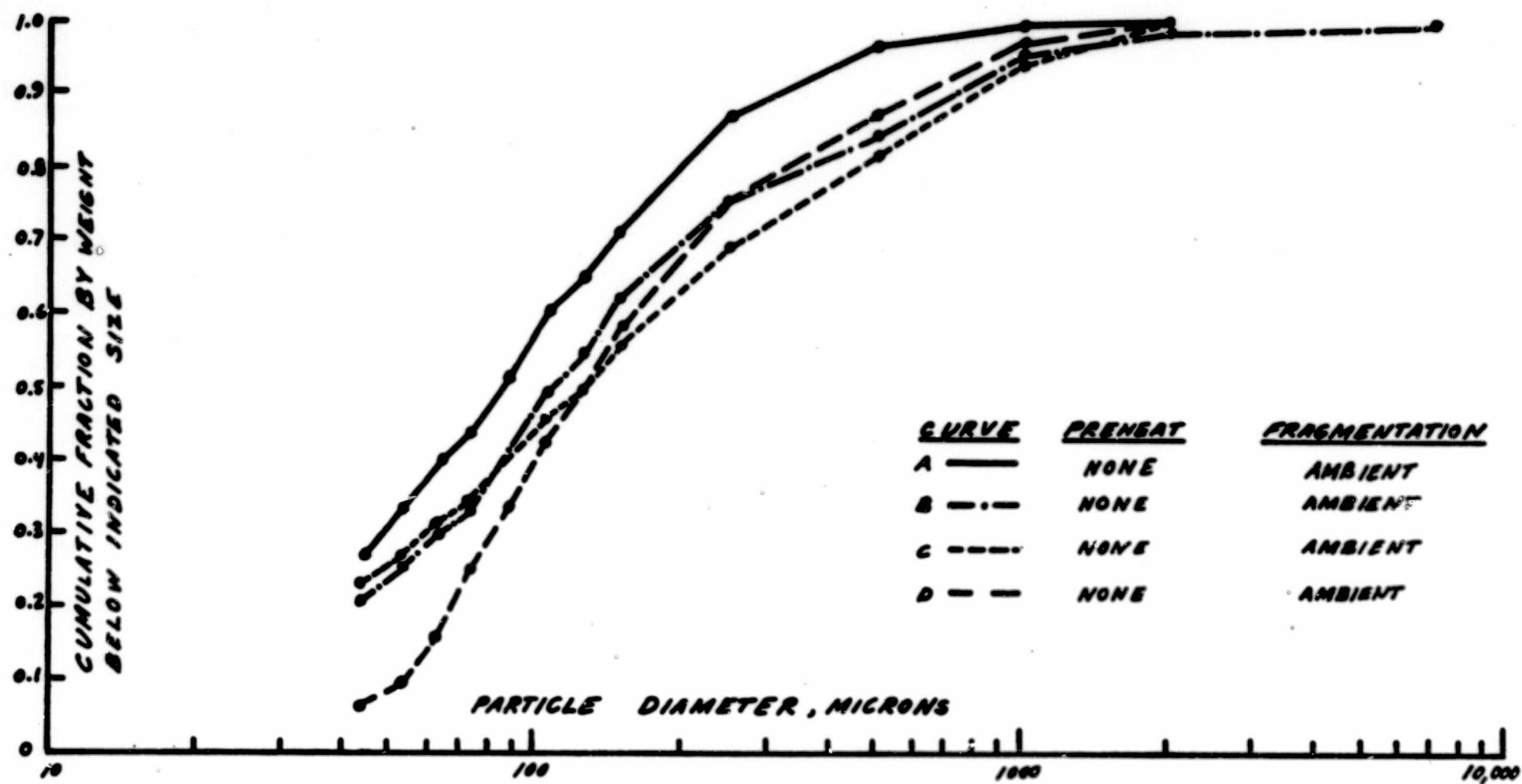
FIGURE - 4

EFFECT OF TEMPERATURE
UPON FRAGMENTATION
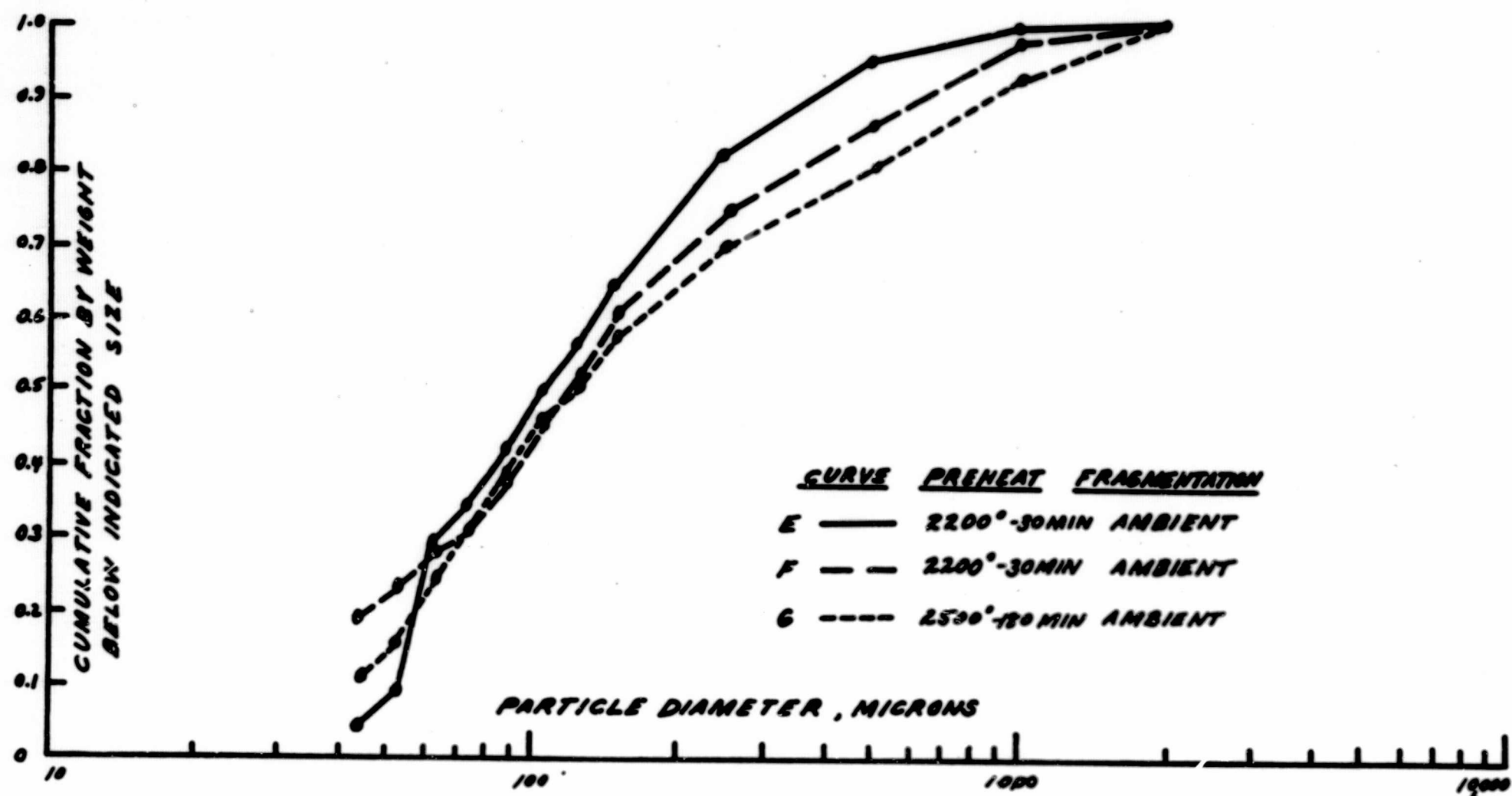
FIGURE 5

EFFECT OF TEMPERATURE
UPON FRAGMENTATION
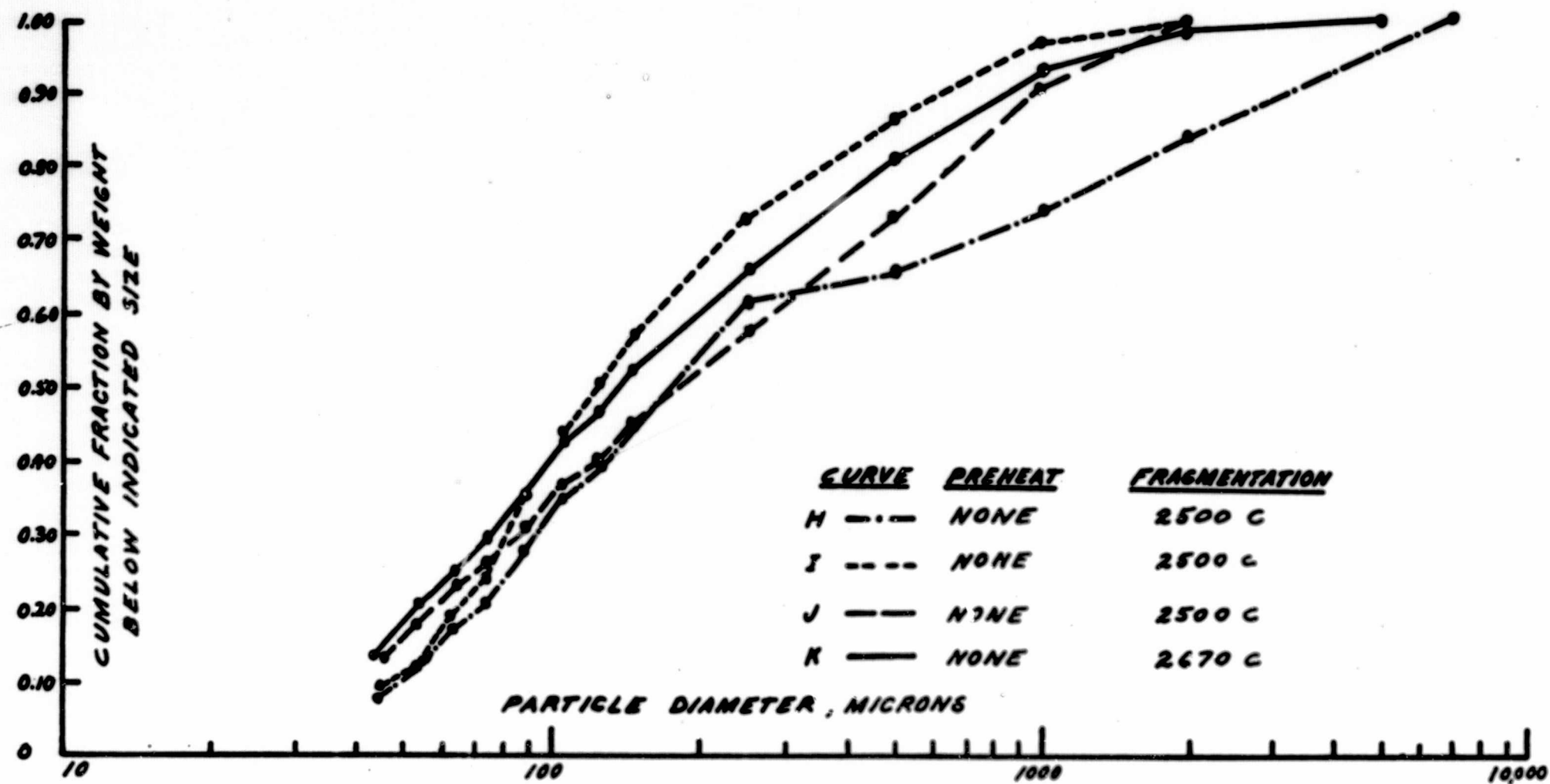
FIGURE 6

EFFECT OF TEMPERATURE
UPON FRAGMENTATION

CURVE	PREHEAT	FRAGMENTATION
L —··—	2200 C -30 MIN	2500 C
M —·—	2500 C -180 MIN	2500 C
N ——	2500 C -180 MIN	2655 C
O ·······	2500 C -180 MIN	2765 C
P — —	2200 C - 30 MIN	2500 C
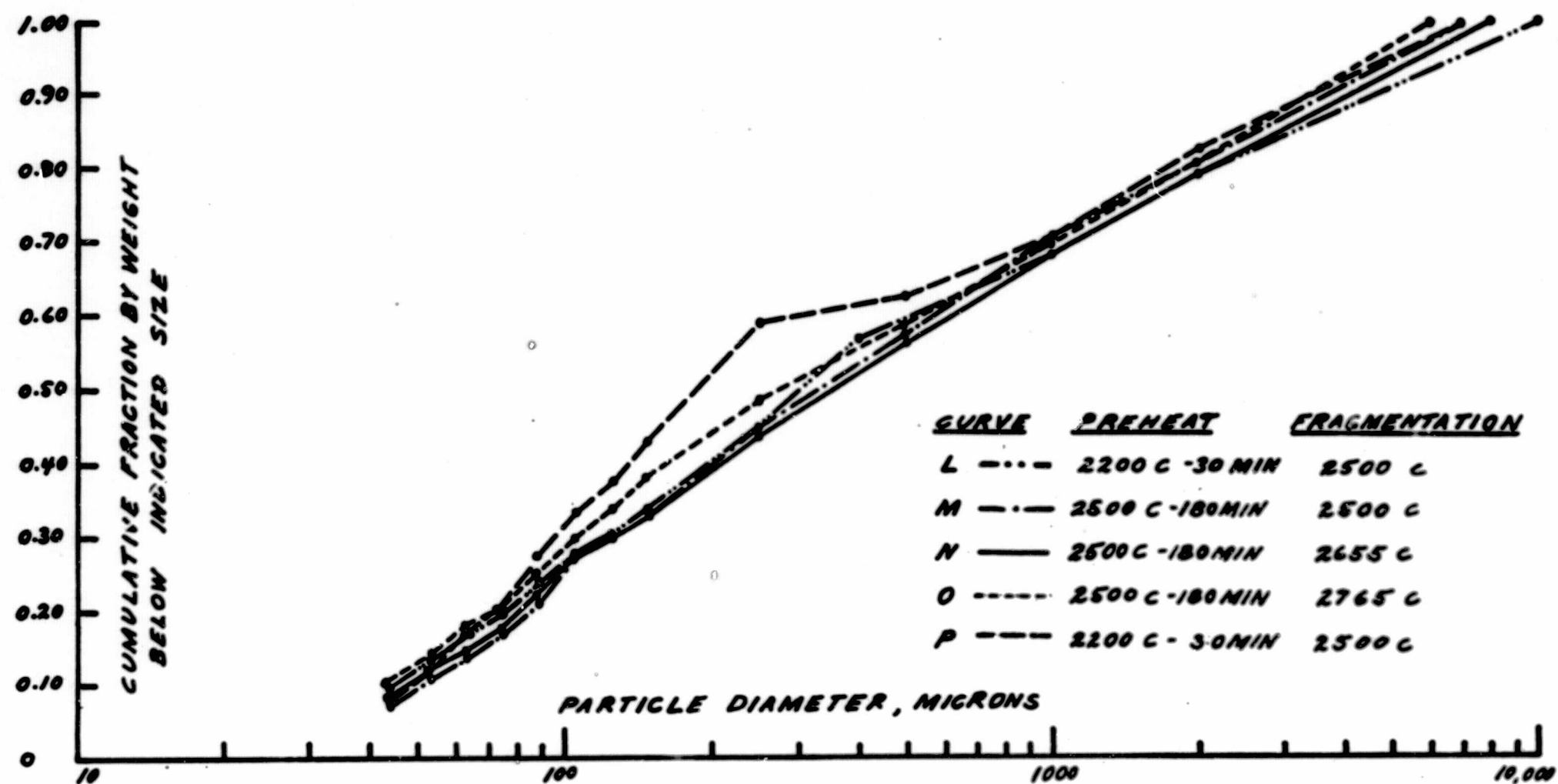
The effect of elevated temperature generally seems to produce a coarser fragmentation. The samples of fuel which have had no pretreatment and are at ambient temperature at the time of fragmentation produce, in general, the finest size distribution followed next by those which were pretreated but were fragmented at ambient temperature. Finally, those which were not pretreated but were fragmented at high temperature had a finer size distribution than those which were both preheated and fragmented while hot. While the preheat temperature affects size distribution, it is affected to a greater degree by the temperature of the fuel at the time of fragmentation. Furthermore, since the reactor will be hot for some time after operation and may actually become overheated prior to destruct system activation, a significantly coarser fragmentation can be expected than that shown by the APG-3 results.

2.   Dispersion of Fragments

The ultimate aim of the destruct systems is to disperse the core in as small fragments as possible over as large an area as possible. The geometry used in placing the four explosive charges in the core mockup in the APG-3 test was such that there was a reinforcing effect midway between the adjacent charges. This reinforcing effect caused most of the core material to be expelled in four jets located midway between the charges. A fifth jet along the reactor axis from the nozzle end also occurs but probably contains considerably less material than the four radial jets. The effect of this charge geometry is shown in Figure 7.

At this point it should be noted that the flight configuration of a high explosive destruct system will not emplant the four charges parallel to the reactor axis. These charges must be placed at an angle to the axis because the design of the propellant tank and upper engine support structure preclude placing the projectile launchers directly above the engine.[5] The effect of non-parallel charge emplacement cannot be predicted. Thus, it is not certain whether or not a similar jetting action will occur in a flight-configured destruct system. One cannot be certain that the fragment size distribution associated with this effect, will remain unchanged.

-13-

FIGURE 7

HORIZONTAL DISPERSION OF CORE MASS
FROM APG-3 TEST (SINGLE QUADRANT)

-14-
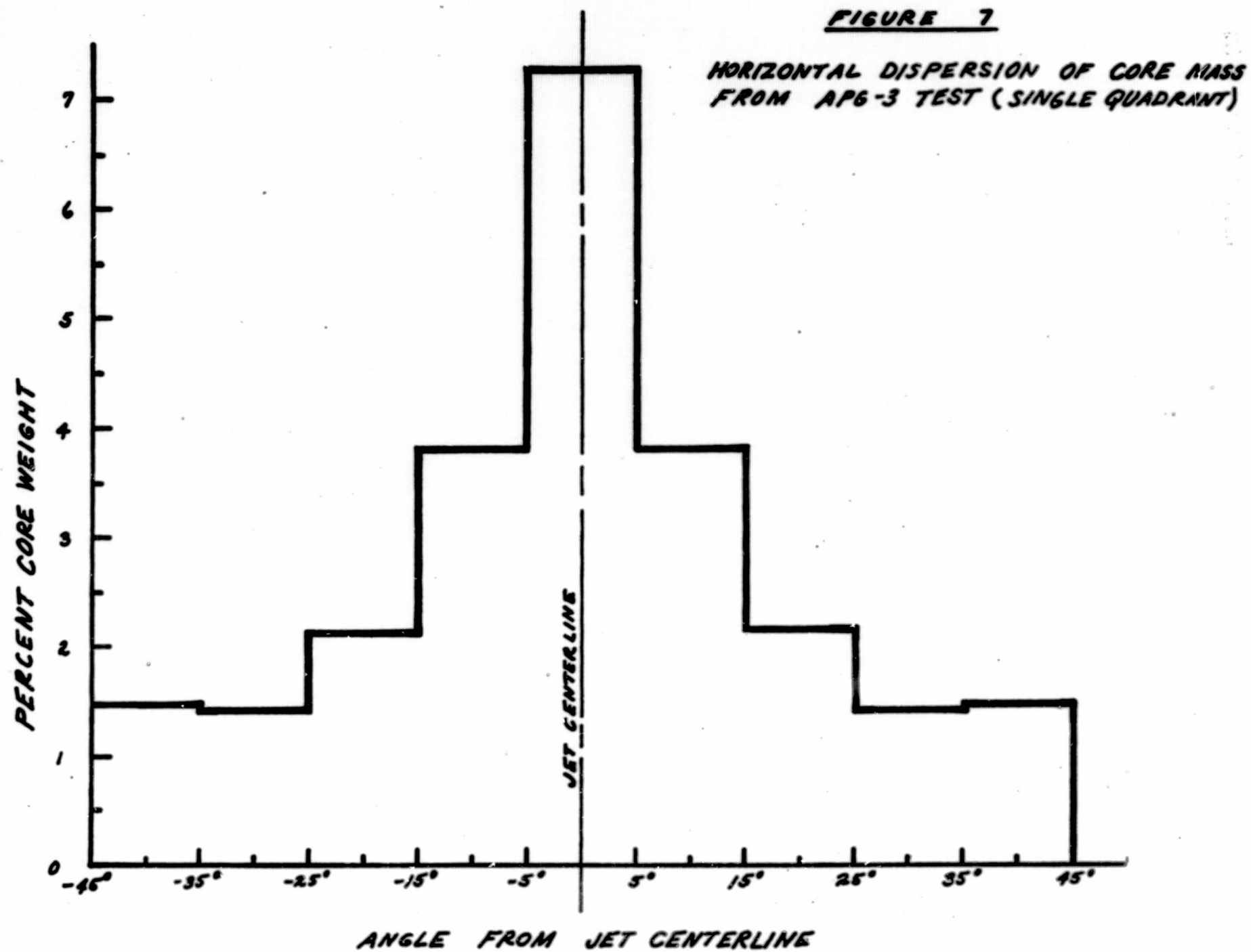
Data from the APG-3 test indicate that the size distribution
of the material in the jets differs from that outside the jets.
Figure 8* shows the mass median diameter of the material
collected following the APG-3 destruct. As can be seen, the
size distribution varies depending upon the sample location
in relation to the jet location and distance. Future scale
model and full size testing is planned[9] to determine the ef-
fect of explosive charge geometry, weight, number of charges,
and detonation timing upon size and radial distribution of
debris.

The effect of non-isotropic ejection of fragments from the core
is to preferentially deposit significantly greater amounts of
debris in some locations than in others. For example the single
jet over the APG-3 test pad contained 7.25% of the core weight
in the 10° sector centered about the jet centerline; in the 10°
sectors centered 45° away from the jet centerline only 1.5% of
the core mass was found. If the dispersion were uniform each
10° sector would have contained 2.78% of the core weight.
Thus destruct of a reactor in space, oriented such that a jet
is pointing downward, would result in a ground deposition
along the centerline of the debris footprint on the ground 4.85
times greater than if the jets are rotated by 45° at the time of
destruct. In the latter case the effect would be to increase
the deposition of debris on the ground closer to the edge of
the footprint.

3.   Fission Product Distribution

The high explosive test data[10] show that the uranium content
of the core debris increases in the size range about the original
bead size in the fuel matrix. Figures 9 and 10 shows the ratio
of uranium weight fraction to graphite weight fraction of the debris.
The sharp peaking which occurs between 50 and 300 microns in-
dicates that in these sizes a greater fraction of the material is
fuel beads with some graphite matrix attached than in other size

---

* Data collected and analyzed by the United States Naval Radio-
logical Defense Laboratory, San Francisco, California.

-15-

FIGURE 8

MASS MEDIAN SIZE VS DISTANCE
FROM GROUND ZERO AND POSITION
IN JET* AP6-3

MASS MEDIAN DIAMETER - MICRONS

ON JET CENTERLINE
45° FROM JET CENTERLINE
* DATA SUPPLIED BY USNRDL

DISTANCE FROM GROUND ZERO -FEET
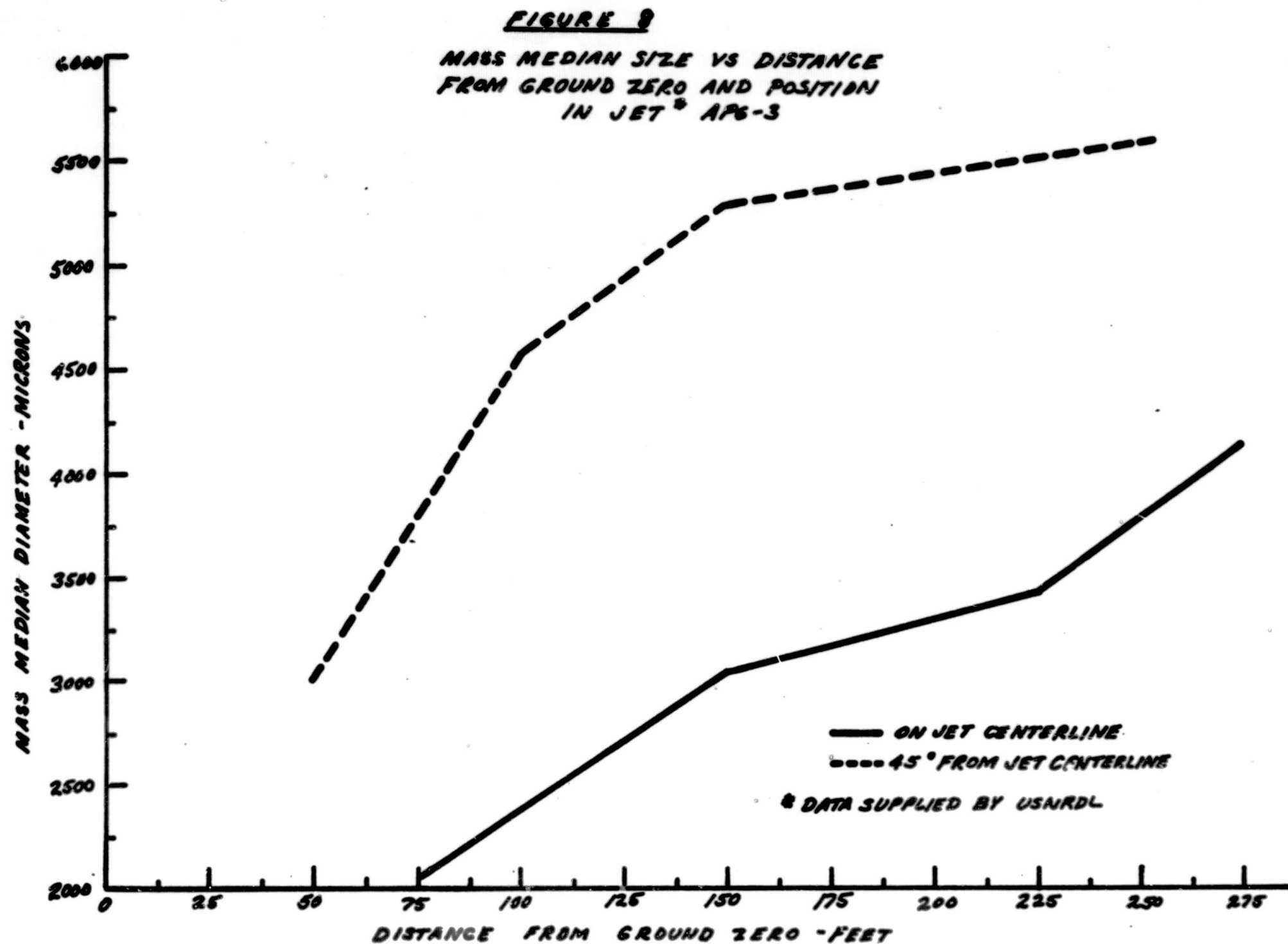
FIGURE 9

URANIUM DISTRIBUTION IN DEBRIS
FLUOROMETRIC ANALYSIS -APG-3

RATIO URANIUM WEIGHT FRACTION TO GRAPHITE WEIGHT FRACTION

PARTICLE DIAMETER -MICRONS

-17-

FIGURE 10

URANIUM DISTRIBUTION IN DEBRIS
GAMMA COUNTING - APG -3

PARTICLE DIAMETER - MICRONS

RATIO URANIUM WEIGHT FRACTION TO GRAPHITE WEIGHT FRACTION
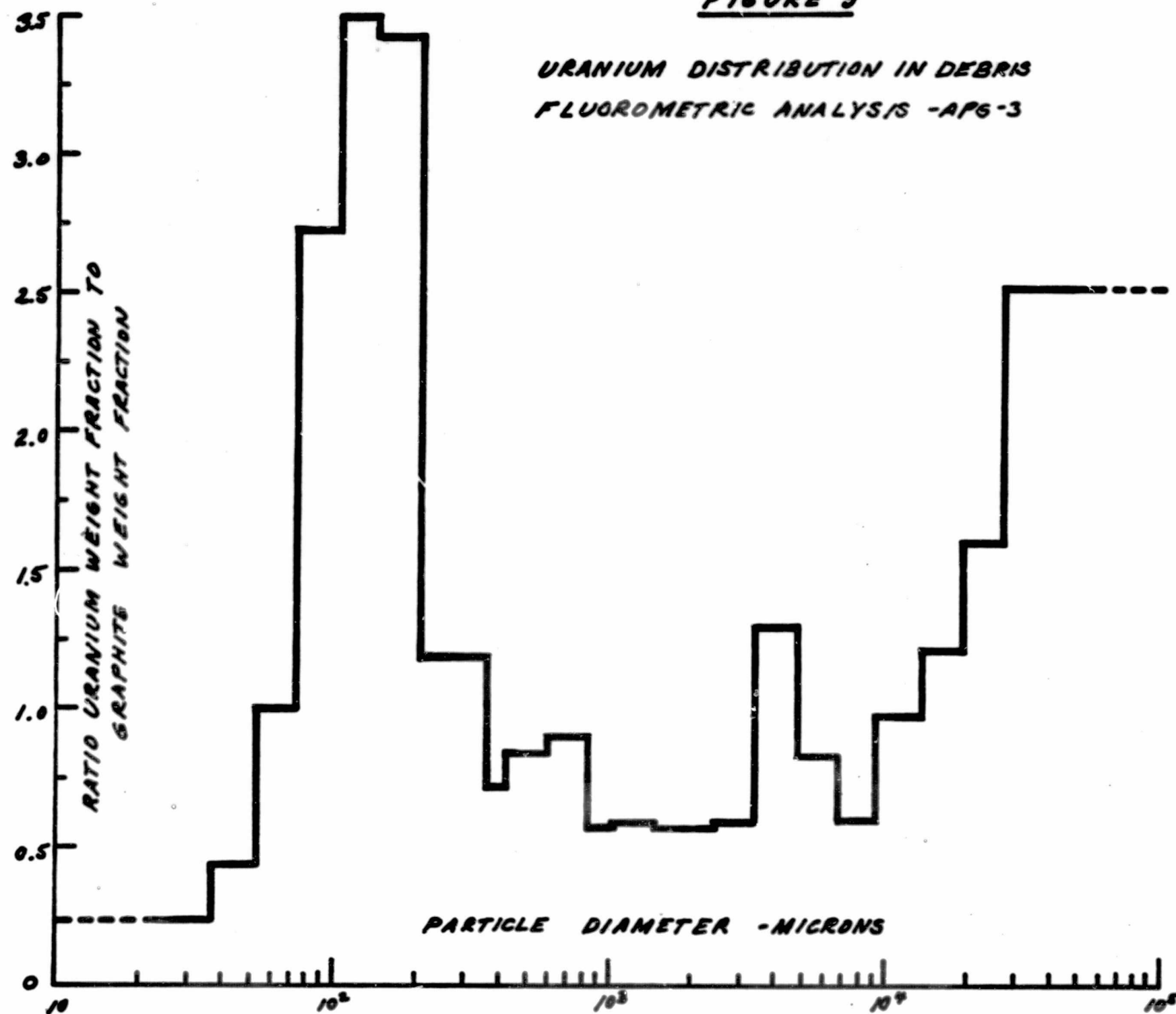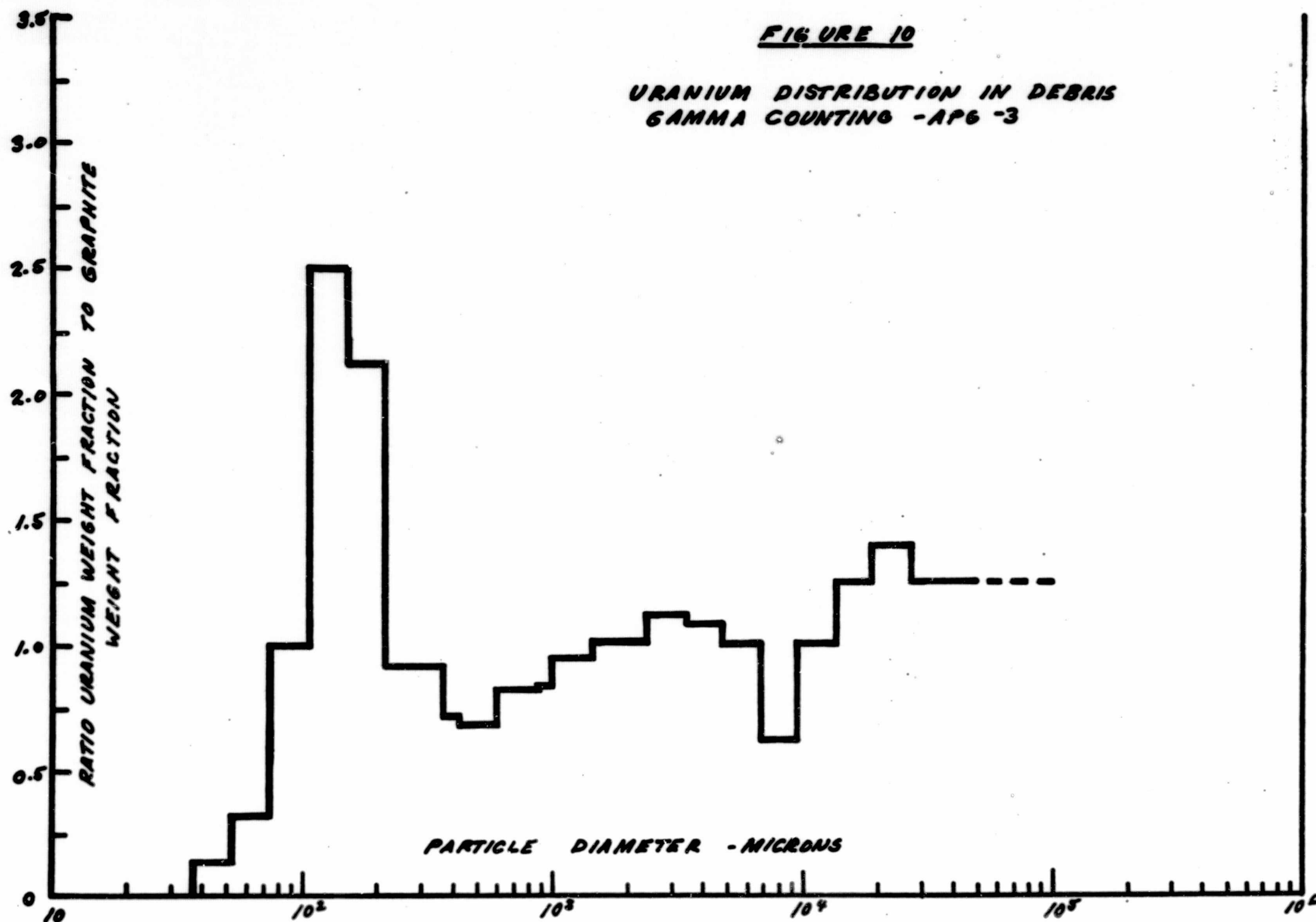
ranges. This would suggest that the specific activity of particles in this size range should be greater than for other size ranges.

However, as mentioned previously, this test did not indicate the effect of reactor temperatures. The LASL series of experiments with the one-inch fuel samples shows that temperature plays a significant role in the uranium distribution.

Figures 11 through 14 show that temperatures on the order of $2200^{\circ}C$ for 30 minutes do not significantly reduce the peaking of uranium content in the fragment sizes near the bead size. Temperatures near or above $2500^{\circ}C$ even for times on the order of a few minutes significantly reduce this peaking. In fact a reasonably uniform uranium fraction with size is observed from these tests. The melting point of uranium dicarbide is $2400^{\circ}C$. Thus, when the temperature is maintained at $2200^{\circ}C$ little or no migration of the UC_2 occurs. However, at $2500^{\circ}C$, migration of the UC_2 occurs to a much greater extent, (possibly by dissolution of the pyrographite coating in molten UC_2) thereby reducing the non-homogenity of the fuel. Additionally, if fragmentation occurs while the reactor is at $2500^{\circ}C$ the molten UC_2 can be more easily dispersed. Normal operating temperature in the reactor is such that some diffusion may occur but melting of the UC_2 should not take place and, hence, there should be no significant effect upon the uranium distribution from a high explosive destruct. However, malfunctions can cause reactor over-heating and fuel bead core melting which would alter the distribution.

Since the explosive destruct system is primarily intended for use in the event of a malfunction of the reactor, it is reasonable to expect that conditions favoring increased fuel migration would exist. Because of the probability of this increased migration of fuel it is believed that the safety analysis of the reentering engine debris need not consider specific activity of debris in certain size ranges higher than the mean for the core.

FIGURE II

EFFECT OF TEMPERATURE
UPON URANIUM DISTRIBUTION

CURVE	PREHEAT	FRAGMENTATION
A ————	2200 C 30MIN	AMBIENT
B ————	2200 C -30MIN	2500 C
C - - - -	NONE	AMBIENT
D —·—·—	NONE	2500 C

LOG-MEAN PARTICLE DIAMETER - MICRONS
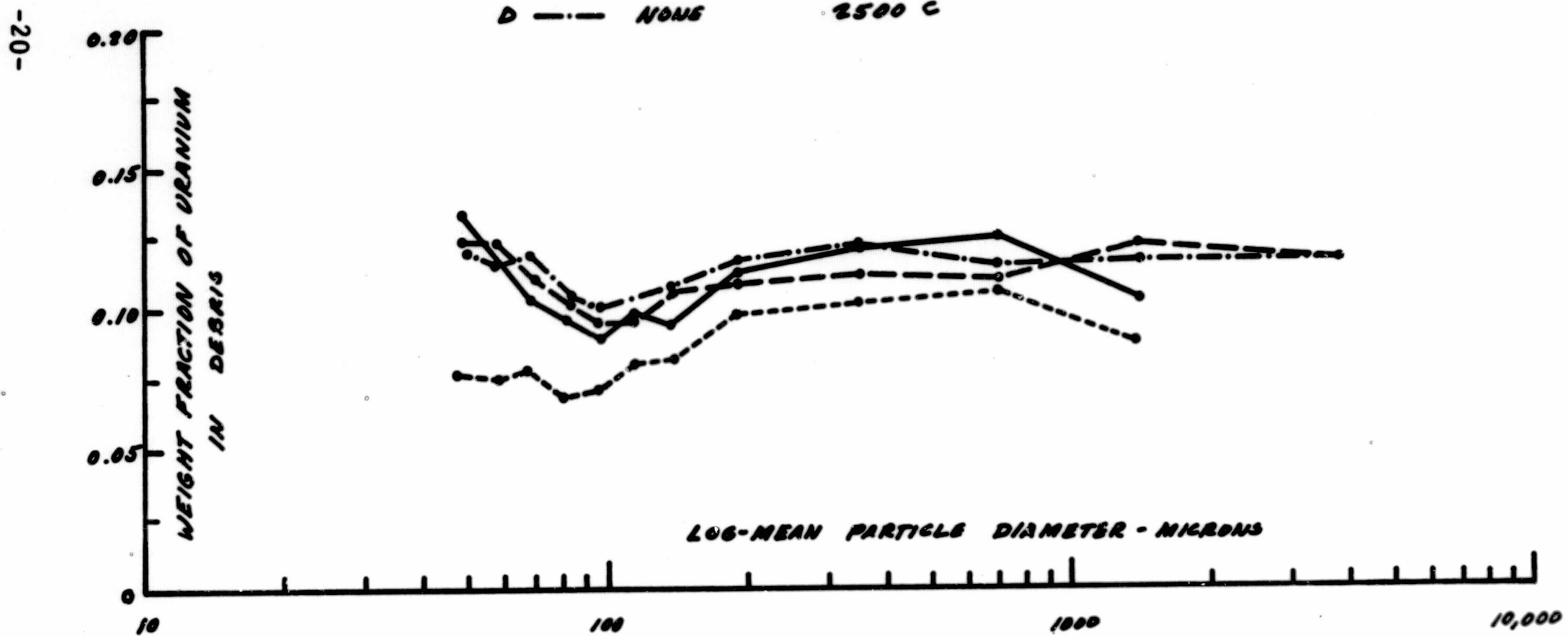
FIGURE 12

EFFECT OF TEMPERATURE
UPON URANIUM DISTRIBUTION

CURVE	PREHEAT.	FRAGMENT
E ————	NONE	AMBIENT
F ———	NONE	AMBIENT
G -----	NONE	AMBIENT
H —··—	2200C-30MIN	AMBIENT

WEIGHT FRACTION OF URANIUM IN DEBRIS

LOG-MEAN PARTICLE DIAMETER -MICRONS
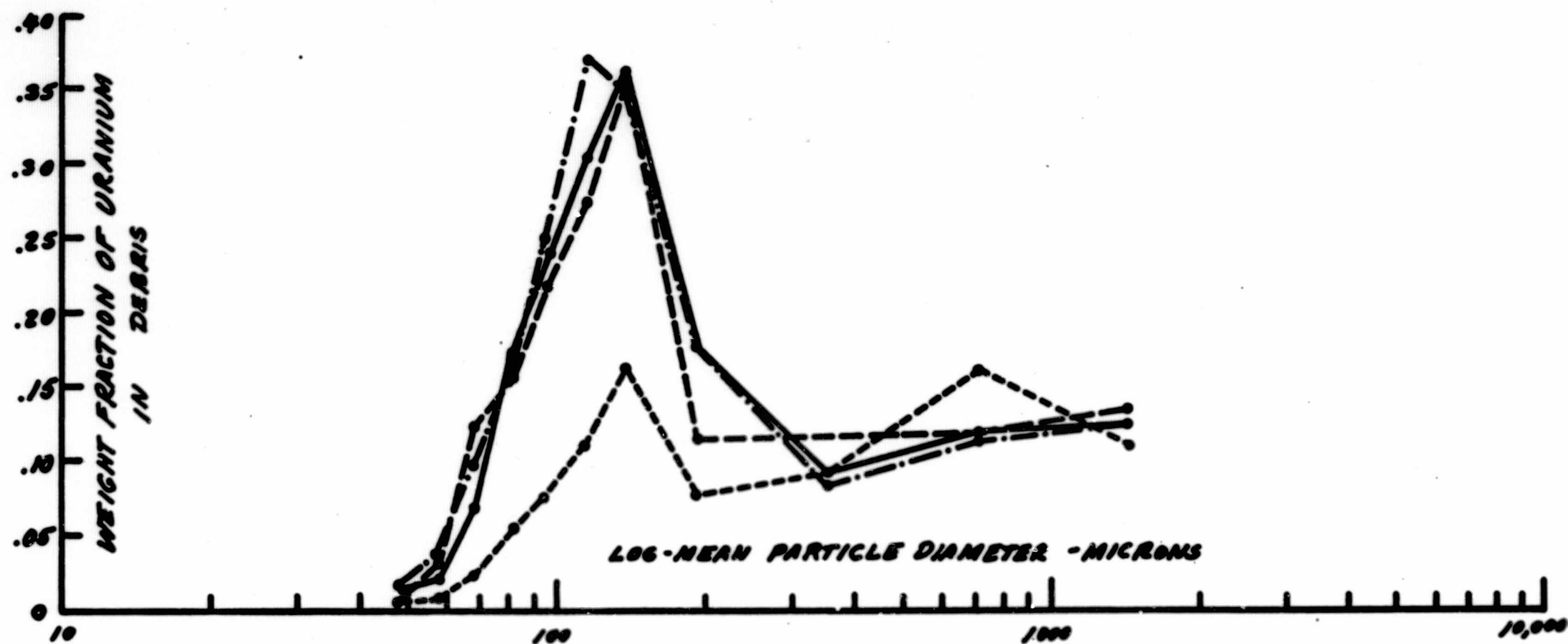
FIGURE 13

EFFECT OF TEMPERATURE
UPON URANIUM DISTRIBUTION

CURVE	PREHEAT	FRAGMENT
I ———	2200°C-30MIN	2500°C
J ———	NONE	2500°C
K ----	NONE	2500°C
L —··—	2500°C-40MIN	AMBIENT

WEIGHT FRACTION OF URANIUM IN DEBRIS

LOG-MEAN PARTICLE DIAMETER - MICRONS
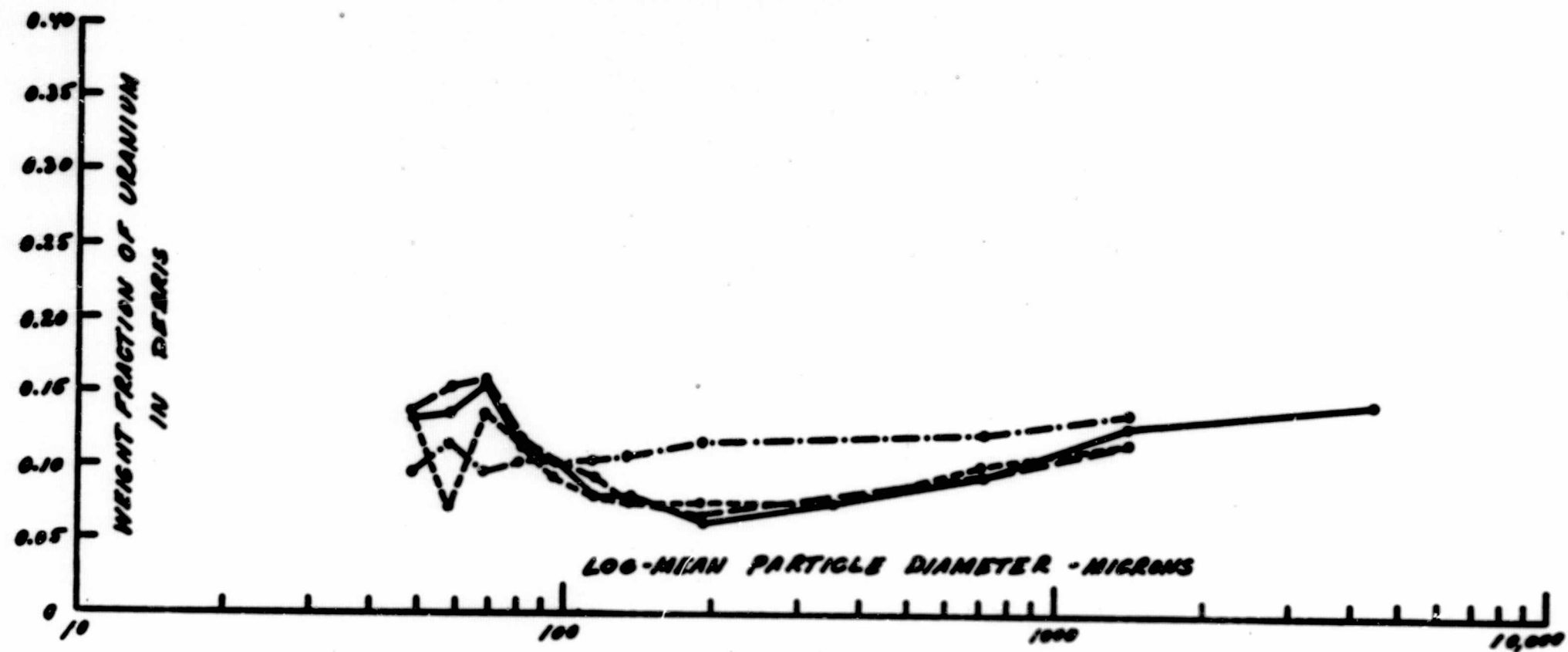
FIGURE 14

EFFECT OF TEMPERATURE
UPON URANIUM DISTRIBUTION

CURVE	PREHEAT	FRAG TEMP
M ————	2500°C 180MIN	2800°C
N — —	2500°C-170MIN	2655°C
O -----	2500°C-10MIN	2765°C
P —·—	NONE	2670°C
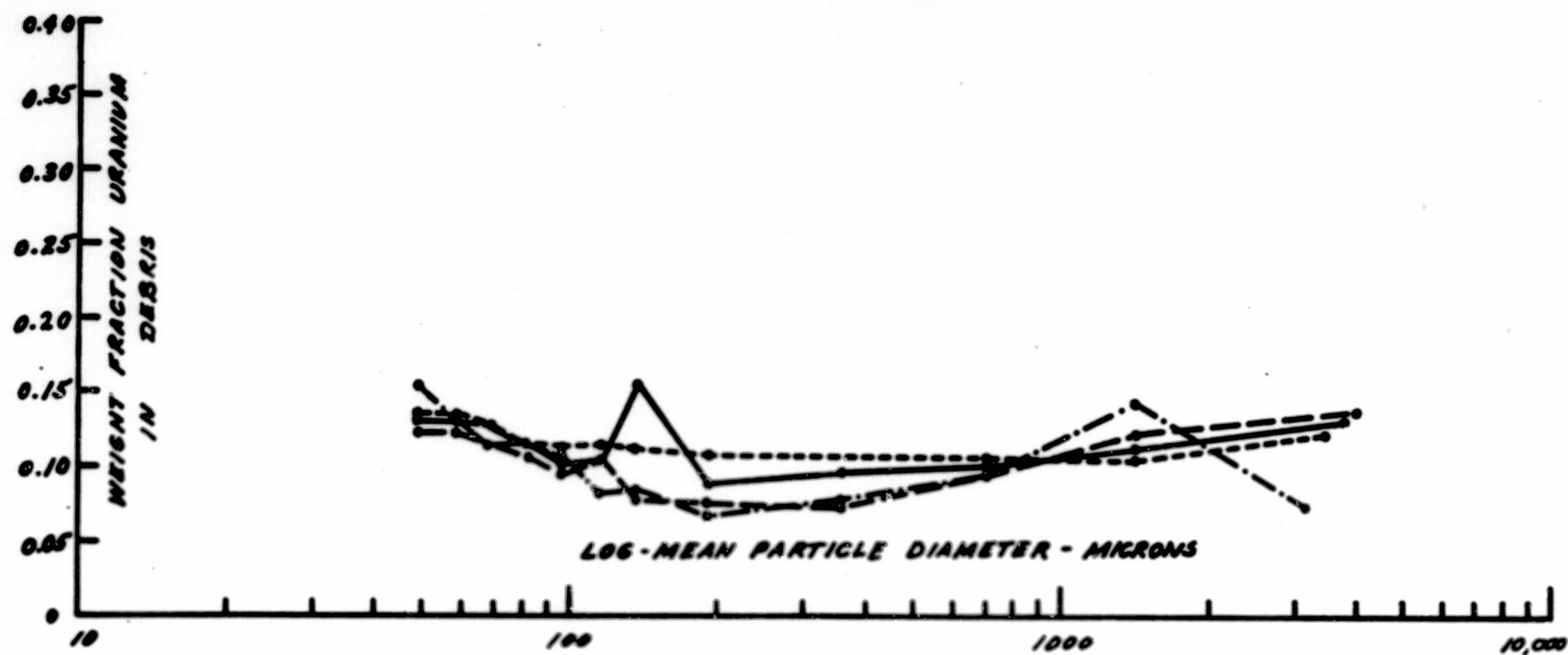
4.   Solubility of Fission Products

No solubility data on specific fission products is available for debris produced by a chemical high explosive destruct. Such data could be obtained by fragmenting a portion of a fuel element from one of the NERVA or KIWI reactor tests conducted at NRDS. Data obtained in this manner would include the effect of normal operational temperature upon fuel and fission product diffusion.

B.   NUCLEAR DESTRUCT SYSTEMS

The concept of the nuclear destruct system is to create a nuclear excursion of sufficiently short period that a large amount of energy is generated in the fuel material causing a high local temperature. This high temperature causes melting and vaporization of the UC_2. The attendant high vapor pressure associated with the high temperature causes fragmentation of the matrix.

The method of producing the transient could be either by rapid drum rotation or by injecting a large amount of moderating material into the reactor core. The method of injecting the material and the moderator material itself has not been determined.

The ability of a nuclear destruct system to fragment the core has not been demonstrated. However, the KIWI Transient Nuclear Test data provides some indication as to the capability of this concept, as do irradiation tests on fuel samples exposed to other short period transients. The KIWI-TNT test was carried out with a modified KIWI reactor. In most construction details the reactor was similar to a normal KIWI engine: the major modifications were in the external structures and control drum actuators. By rapidly rotating the control drums, a nuclear transient with a period of about 0.6 msec and an energy release of 3×10^{20} fissions was achieved.

It should be emphasized that the KIWI-TNT was not intended to simulate a nuclear destruct system; however, the data from this test is useful for estimating the characteristics of a nuclear destruct in the absence of more appropriate data.

The data from KIWI-TNT that are useful for characterizing nuclear destruct are the weight and particle number distributions as a function of particle size, the dispersion of fragments, the fission product distribution as a function of size and the fission product solubility.

1.   Fragment Size Distribution

Figure 15[11] shows the size distribution of the debris recovered following the KIWI-TNT test. The mass median diameter is 40,000 microns, Figure 16[11] shows the distribution of the estimated number of particles as a function of size and the average particle weight. The KIWI-TNT test, like the high explosive destruct tests did not demonstrate the effect that normal operating temperatures would have upon the fragmentation characteristics. However, the high temperatures generated by the transient itself may have produced the significant effects.

The KIWI-TNT test did provide an opportunity to irradiate samples of other fuel types and to determine the energy release required to cause complete fuel breakup. In general, it was found that the fragmentation of these fuel samples was quite uniform[11] and resulted in a particle size of about 1/16-inch (1590 microns). Energy deposition corresponding to about 5×10^{14} fissions/gram caused bead damage. This damage, depending upon the fission density, varied from small cracks in the bead coating to large or multiple cracks with the loss of some UC_2 from the bead core. Fission densities on the order of 1.5×10^{15} fissions/gram[12] are sufficient to cause fracturing of all beads and the loss of the UC_2 core.

Because of the strong dependence of bead fracturing upon the fission density, the effect of engine temperatures which cause any significant UC_2 migration would be to reduce the fission density for a given excursion. Thus, a larger excursion would be required.

FIGURE 15
KIWI-TNT SIZE DISTRIBUTION

WEIGHT PERCENT BELOW INDICATED SIZE

PARTICLE SIZE - MICRONS

FIGURE 16

NUMBER OF PARTICLES AND
WEIGHT PER PARTICLE FROM
KIWI - TNT TEST

- 27 -
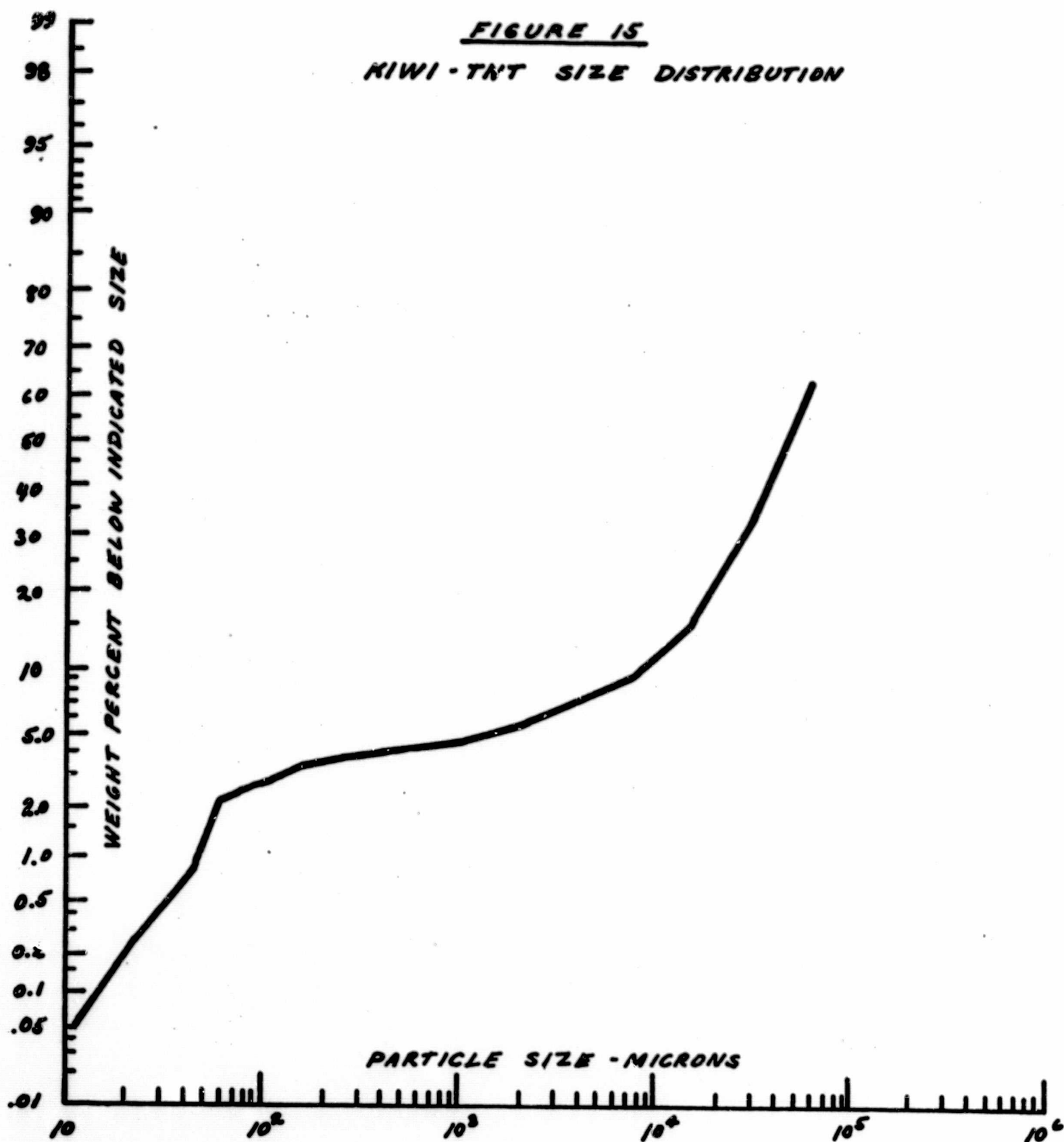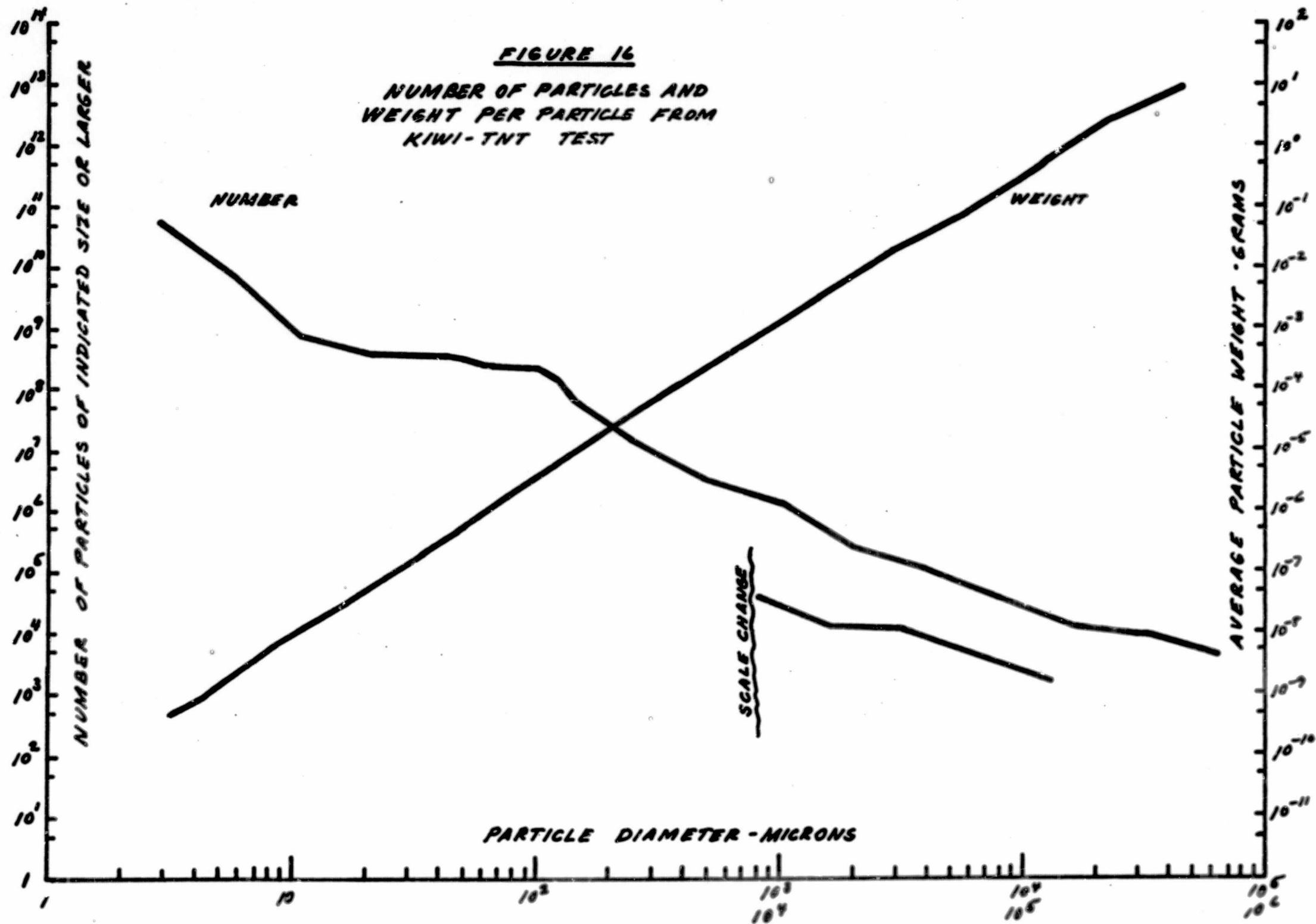
In the KIWI-TNT, the fission density was above the threshold for bead fracturing for all but about 4 inches at the ends of the core. Thus, for a KIWI-type reactor the required energy release to completely fragment the core is estimated to be about 1×10^{21} fissions[11]. Additional energy release would be required if significant UC_2 diffusion occurs, however.

Changes in fuel bead and element loading would also effect this estimated energy release. Capsule experiments from KIWI-TNT[12] indicate larger bead sizes with thinner coatings require less energy for fragmentation. Increasing the uranium loading fractions also decrease the energy required for breakup.

2. Dispersion of Fragments

The dispersion of particles from the KIWI-TNT was reasonably uniform radially as evidenced by both photographic records of the test and by the recovery of the larger fragments of the reactor core which were unaffected by the 15 to 20 knot wind which existed at the time of the test. These larger particles and pieces of the reactor vessel were found uniformly distributed about the origin.

However, whether an operational nuclear destruct system would give this same uniform distribution is subject to conjecture. This question is raised primarily due to the probable manner in which the transient will be initiated. In the KIWI-TNT the transient was initiated by rapidly turning twelve control drums at the core periphery. The resulting energy release was generally angularly uniform. However, a flight nuclear destruct system which produces the excursion by the injection of moderator into various parts of the core could produce local power peaking. Depending upon the severity of this peaking, shock wave reinforcement at certain locations could occur producing a non-uniform dispersion as was produced in the APG-3 test. Since this non-uniform dispersion is based only on conjecture at this time, it will be assumed that the dispersion of particles will be more or less uniform and that a nuclear destruct system can be designed that will cause fragmentation and dispersion at least as great as that produced in the KIWI-TNT test.

3. Fission Product Distribution

As mentioned previously, the mechanism for fragmentation[12,13] by a nuclear excursion is the generation of a high-internal vapor pressure and thermal stresses which cause the fuel bead to "explode" causing fragmentation of the fuel matrix. As the beads and matrix fracture, the UC_2-vapor or liquid is released. This vapor and liquid is free to condense and freeze on the surface of matrix particles. Analysis of KIWI-TNT data[13] indicates that about 2/3 of the fission products were vaporized while only about 5 to 20% of the core material was vaporized. Radiochemical analysis of the KIWI-TNT debris shows that the activity associated with the particles is nearly proportional to the square of the particle diameter[13]. This indicates a dependence of activity upon the surface area of the particle.

This surface deposit of activity is desirable since any ablation of the particle surface due to aerodynamic heating during the re-entry phase should substantially reduce the activity associated with the particle. The extent of this reduction remains to be demonstrated.

4. Solubility of Fission Products

The U.S. Naval Radiological Defense Laboratory[14] obtained a number of samples from the KIWI-TNT test to determine the solu-bility of the contained fission products. The results of these solubility tests, although not representative of the solubility of fission products from a nuclear destruct in space because of the effect of reentry heating, can be used to indicate at the degree of solubility to be expected. Table II shows the results of solubility tests in distilled water and 0.1N HCl. The solubility data in 0.1N HCl is believed to approximate the solubility in body fluids.

USNRDL obtained other data regarding the degree of fractionation of fission products and gross activity decay rates. This data, however, has little application to this study and, consequently, is not discussed here.

TABLE - II

PERCENT OF RADIONUCLIDES LEACHED FROM KIWI-TNT
DEBRIS UNDER VARIOUS CONDITIONS

Sample	Ground Filter Unit			Fallout*	
Leach Solution	Distilled Water	0.1N HCl	0.1N HCl	0.1N HCl	0.1N HCl
Radionuclide					
Sr^{89}	94	98	7	16	20
Sr^{90}	93	96	5	13	20
Y^{91}	58	84	5	11	19
Zr^{95}	<7	6.7	3.5	1	1.0
Mo^{99}	46	40	--	--	--
Ru^{103}	<21	<77	14	29	17
Ru^{106}	41	51	21	28	20
Te^{131}	--	--	--	--	--
I^{131}	66	55	--	--	35
Te^{132}	64	74	--	--	--
Cs^{136}	28	30	0	--	--
Cs^{137}	34	31	20	26	28
Ba^{140}	77	87	88	16	27
Ce^{141}	--	--	--	--	--
Ce^{144}	43	60	15	17	25

* 701 - 1400 Microns.

The analysis of samples taken from the ground air sampling
filter units indicate that the samples are enriched by about
a factor of 20 in strontium and up to 30 - 40 in iodine and
tellurium whereas the fallout samples which were in the size
range of 700 to 1400 microns were more depleted in these
elements. Figure 17 shows the ratio of Sr-89 to Zr-95 vs.
the ratio of I-131 or Te-132 to Zr-95. In general, the larger
the particle the greater the depletion of strontium and iodine.

The samples collected on the air filter unit on the ground and
from the cloud resulted in larger amounts of fission product
leaching than did the larger fallout samples. Since the
particles which are small enough to be airborne do not contain
a significant fission product inventory the high solubility ex-
hibited is not indicative of severe organ doses[4]. The larger
particles with larger inventories do not exhibit significant
fission product solubilities.

FIGURE 17

FISSION PRODUCT FRACTIONATION
IN KIWI-TNT DEBRIS

-32-
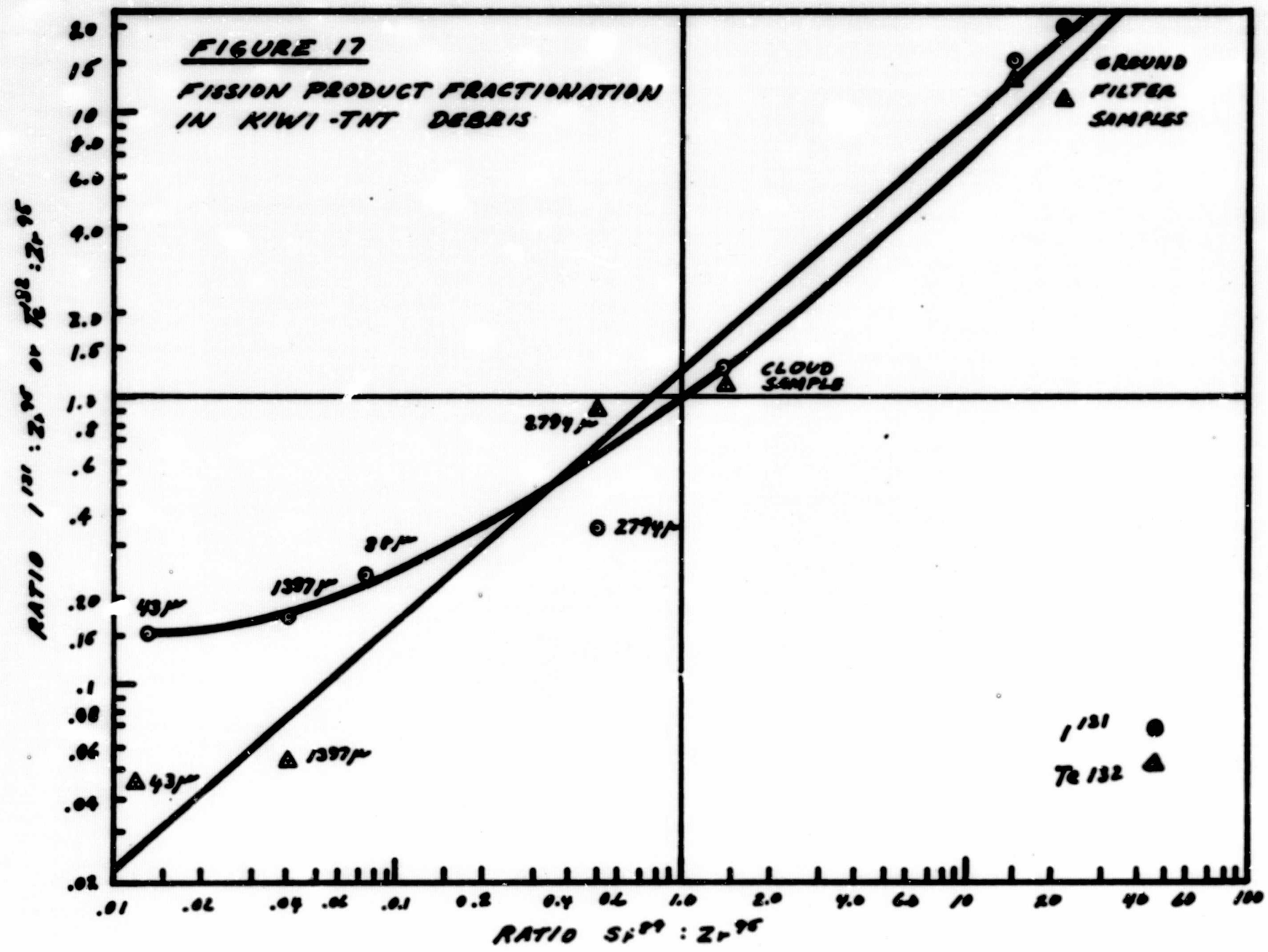
III. PARTICLE EXPOSURE

The ultimate objective of this report is to present a comparison of the possible doses delivered as a consequence of both a nuclear and a high explosive destruct of a nuclear rocket reactor. Since the reactor operating time and power level will be the same for both destruct systems for any given mission, the initial fission product inventory will be identical also. After destruct system activation a number of differences exist in the characteristics of the debris, however. Unfortunately, the magnitude of many of these characteristics is unknown and, consequently, it will be assumed that the differences in the characteristics that are to be considered are:

    a.   The size and number distribution of particles

    b.   The dispersion of particles, i.e., uniform vs. non-uniform dispersion

    c.   The fission product inventory added by the nuclear destruct

    d.   The fission product distribution in the particles of debris

    e.   The fission product inventory lost by vaporization.

The comparison of the consequences of each destruct must be evaluated in terms of both the dose delivered and the probability of exposure.

The exposure situations to be considered are:

    a.   External whole body exposure

    b.   Gastrointestinal exposure
        (1) by inhalation
        (2) by ingestion

    c.   Lung exposure

    d.   Skin external contact exposure

The relationships for determining the exposure probability and dose have been developed and are discussed in previous documents[3,4]. Each exposure route is considered separately below.

A. EXTERNAL WHOLE BODY EXPOSURE

The relative effects of whole body exposure can be estimated using the results from machine computation using the MOREDO program[15] for an averaged world population.[16]

For this comparison the population exposure is adequate to describe the relative exposure obtained for a given destruct system.

The population exposure, $PE_{(j)}$, for size j particle is given by [3]

$$PE_{(j)} = 2\pi M_j \sum_i \bar{n}_i \int_0^\infty SD_{(s,j,i)} ds \qquad (I)$$

where: M_j = total number of particles of size j

$\bar{n}_i$ = mean population density of the ith group

S = distance from source to receptor motion center

$D_{(s,j,i)}$ = dose to receptor from particle

To determine the total exposure a given population will receive, it can be seen that the population exposure is simply proportional to the total number of particles affecting that population. (It is stressed here that this is true only for that single population for which the summation over all age-occupation groups, i, is valid.)

Rearranging equation (I)

$$\phi = \frac{PE_j}{M_j} = 2\pi \sum_i \bar{n}_i \int_0^\infty SD_{(s,j,i)} ds \qquad (II)$$

From the results of a MOREDO calculation with the one region world model[16] the total population exposure for the largest particle size class was

$$PE_{j=1} = 3.93 \times 10^5 \text{ man rad}$$

-34-

The particle density was 1.738×10^{-10} particles/meter^2 over an area of 9.18×10^{13} meters ^{2}; therefore, the total number of particles is

$$M_j = (1.738 \times 10^{-10} \text{ part/m}^2)(9.18 \times 10^{13} \text{m}^2) = 1.59 \times 10^4$$

particles and thus

$$\phi = \frac{3.93 \times 10^5}{1.59 \times 10^4} \quad \frac{\text{Man rad}}{\text{particle}} = 24.7 \text{ man rad/particle}$$

The particle, which was 31,162 microns in diameter, emitted a total decay energy of 5.5×10^{17} Mev from 1 hour after shutdown to infinity. Hence, assuming decay according to the Way-Wigner relationship, the decay rate 1 hour after shutdown was 1.1×10^{17} Mev/hr or $3.06 \times 10^{13} \frac{\text{Mev}}{\text{sec}}$. The energy distribution used in the calculations was from the data of Perkins and King[17] for 1 hour reactor operation and 100 hours after shutdown as shown on Table III. The average energy for this distribution is about 0.88 Mev. However, for impact in Africa for which this report is based, the reactor operating period is only about 500 seconds. Thus, using the Perkins and King data for instantaneous fission for 1 hour after shutdown yields approximately $1 \times 10^{-4} \dfrac{\text{Mev}}{\text{Sec Fission}}$

therefore,

$$\phi = 24.7 \frac{\text{Man rad}}{\text{particle}} \quad \frac{\text{Sec-particle}}{3.06 \times 10^{13} \text{ Mev}} \quad \frac{1 \times 10^{-4} \text{ Mev}}{\text{Sec fission}}$$

$$\phi = 8.07 \times 10^{-17} \text{ man rad/fission}$$

This value of ϕ can be multiplied by the total deposited fission energy to obtain the population exposure.

B.   GASTROINTESTINAL EXPOSURE

The mean number of particles swallowed via the respiratory system per person per unit particle deposition on the ground can be calculated using methods published elsewhere[3,4]. Figure 18 is obtained using these methods and assuming a 2 meter per second wind and the standard man breathing rate.

TABLE - III

ENERGY DISTRIBUTION USED IN MOREDO CALCULATIONS

Energy Range	Average	Decay Energy $\frac{Mev/sec}{Mw-hr}$	Fraction
0 - 0.4 Mev	0.20 Mev	4×10^{12}	0.1409
0.41 - 0.90	0.65	15×10^{12}	0.5287
0.91 - 1 35	1.13	2.6×10^{12}	0.0916
1.36 - 1.80	1.58	5.6×10^{12}	0.1974
1.81 - 2.20	2.00	0.5×10^{12}	0.0176
2.21 - 2.60	2.40	0.65×10^{12}	0.0229
2.61 - 5.13	3.87	0.02×10^{12}	0.0007
	$\overline{E}$ 0.88 Mev	28.37×10^{12}	

FIGURE 18

MEAN EXPOSURE FROM INGESTED
(VIA INHALATION AND SWALLOWING)
PARTICLES OF DEBRIS.
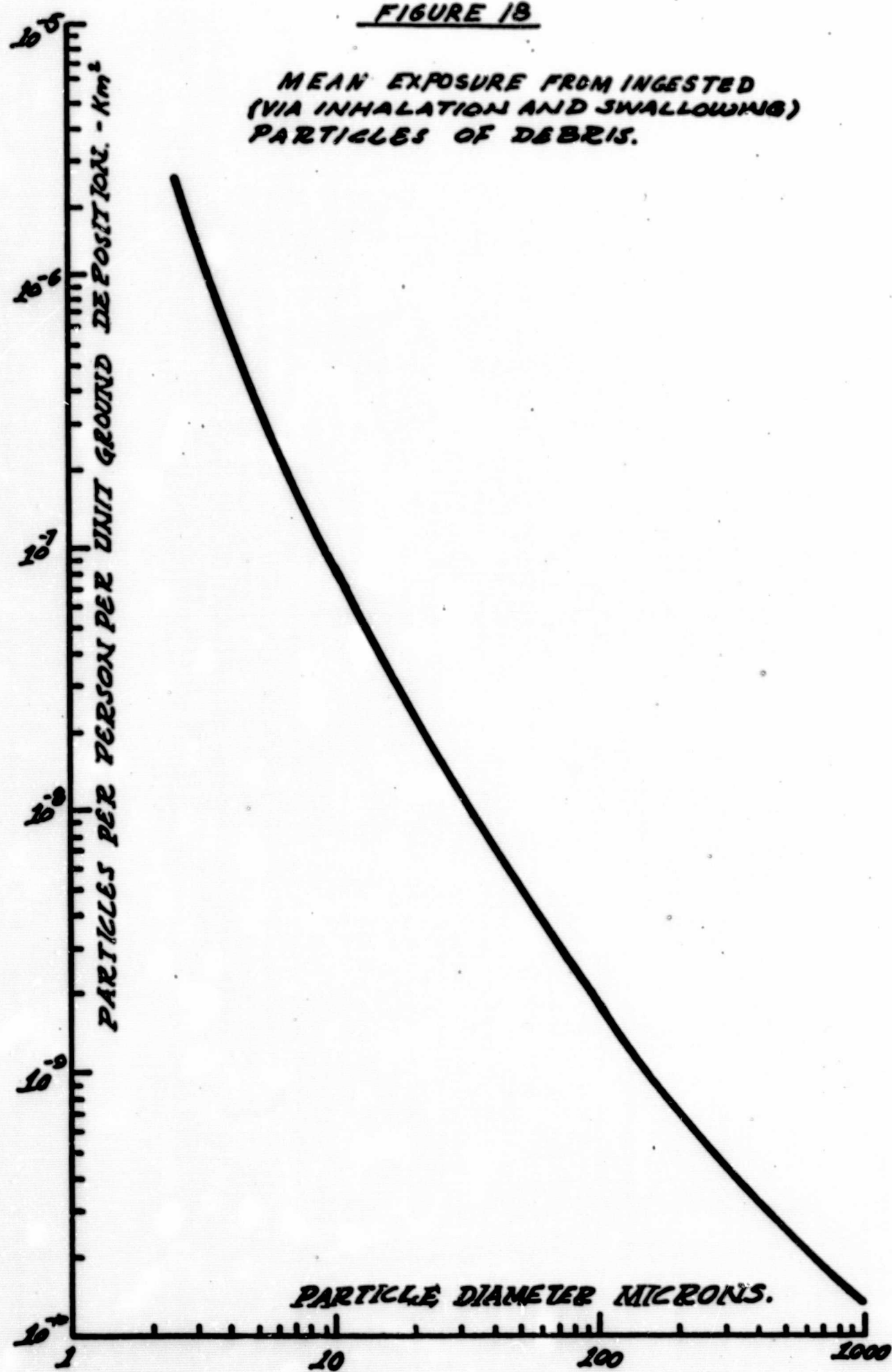
Methods for calculating the mean number of particles ingested via
contaminated food have also been derived[3,4]. However, a number
of factors must be used to calculate the mean particle intake which
are at present not well known. Since the mean particle intake will
vary directly with deposition density of the particle, the mean in-
take will not be calculated.

C.   LUNG EXPOSURE

The mean number of particles per person reaching the lung per unit
particle deposition, $\dfrac{\psi_k}{m_j}$, can be calculated [3,4] to be

$$\frac{\psi_k}{m} = 625 \left(\frac{part}{person}\right) \left(\frac{cm^2}{part}\right) \text{ for 3.1 micron diameter particles}$$

$$\frac{\psi_k}{m} = 4.35 \left(\frac{part}{person}\right) \left(\frac{cm^2}{part}\right) \text{ for 14.1 micron diameter particles}$$

assuming a 2 meter per second wind.

D.   SKIN EXPOSURE

Figure 19 shows the mean number of particles per person per unit
deposition which are expected to strike and stick to the skin. Again,
the methods developed in references (3) and (4) were used to obtain
Figure 19.

-38-

FIGURE 19

DIRECT SKIN CONTACT- MEAN.
DEPOSITION ON SKIN PER UNIT GROUND DEPOSITION.

PARTICLE SIZE, MICRONS.

$\rho = 2.6$
$V_W = 200 \, cm/sec.$
NUDE SUBJECT.

-39-
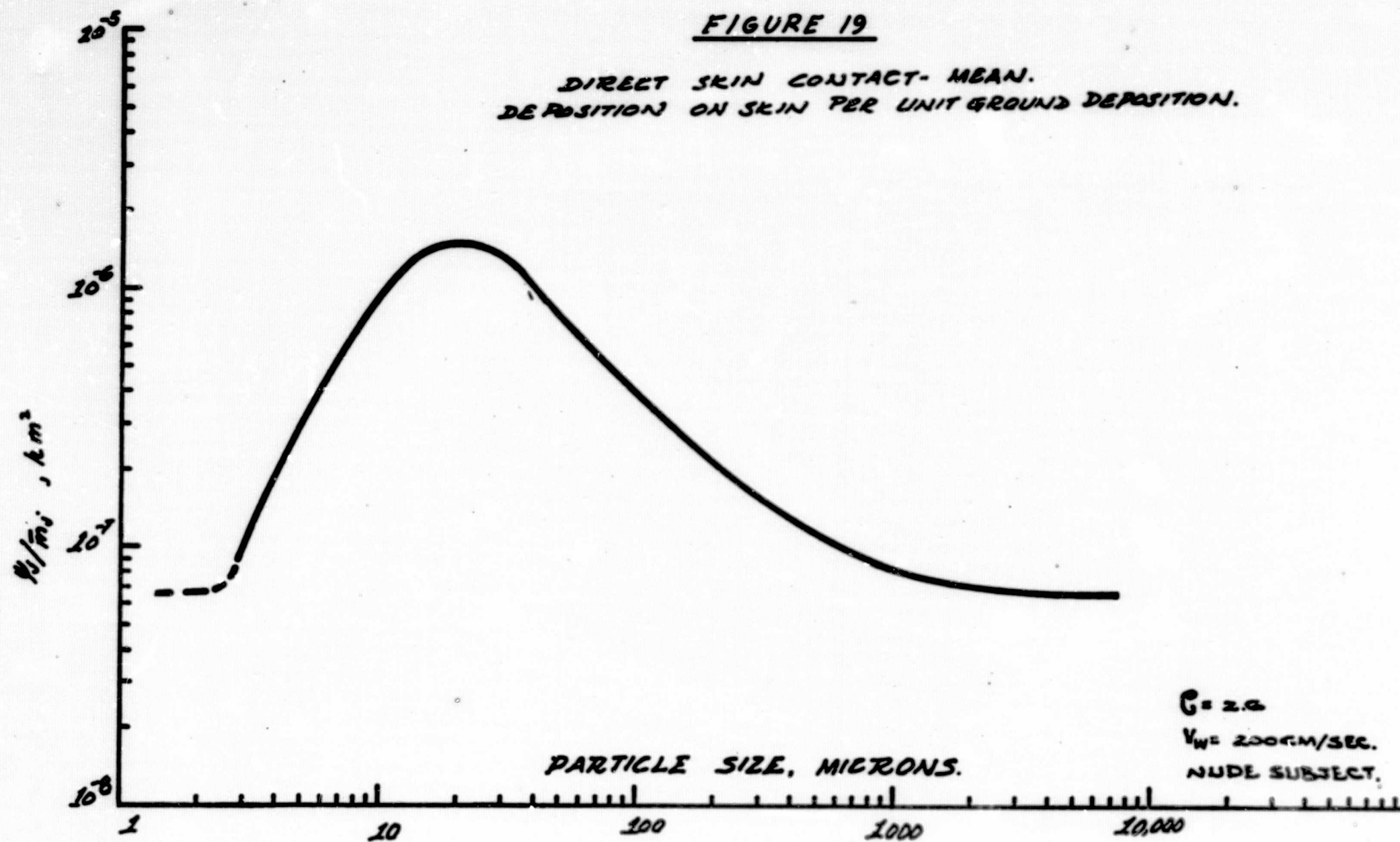
IV. DOSE EVALUATION AND SYSTEM COMPARISON

To evaluate the various doses obtained as a result of nuclear and high explosive destruct it is necessary to define the deposition density of particles, i.e., number of particles per unit ground area for each size class. For sub-orbital destruct, the deposition of particles on the ground will depend upon the altitude of destruct and the velocity vector imparted to each particle at the time of destruct and, hence, the deposition density can only be predicted by application of classical trajectory and reentry calculations. For orbital destruct, impact location cannot be predicted but the deposition of particles will be generally random between latitudes 40 N and 40 S.

For this study the deposition of particles will be assumed to be uniform throughout a rectangular impact area. This impact area as a function of particle size shown on Figure 20 is obtained from data in reference (18). (Later studies[2] will probably show revised impact areas, however, the results of these final studies are unavailable at this time.) Table IV shows the number of particles in each size class while Table V shows the particle number density for high explosive and nuclear destruct.

The particle densities in Table V are used to determine the doses derived following each type of destruct. The particle densities from high explosive destruct can vary from 0.54 to 2.6 times the areal densities given in the table because of the non-uniform dispersion created by the jetting action demonstrated in Figure 7. (See Section II A2).

A failure of the nuclear rocket at 1090 seconds of flight time would allow the particles generated from a destruct of the reactor to impact in South Africa. Thus, the flight profile would account for 586 seconds of booster[18] operation and about 504 seconds of nuclear stage operation. The total number of fissions which have occurred are approximately;

$$504 \text{ sec } (1100 \text{ Mw}) \ 3.16 \times 10^{16} \ \frac{\text{fission}}{\text{Sec-Mw}} = 1.75 \times 10^{22} \text{ fissions}$$

The inventory of each particle from a high explosive destruct can be estimated by assuming the fission products are distributed

FIGURE 20

LAND AREA COVERED BY
FRAGMENTS FROM A NERVA DESTRUCT
AFTER 1090 SECONDS
OF FLIGHT

TOTAL AREA
40°N - 40°S

LAND AREA COVERED - KM²

PARTICLE DIA - MICRONS
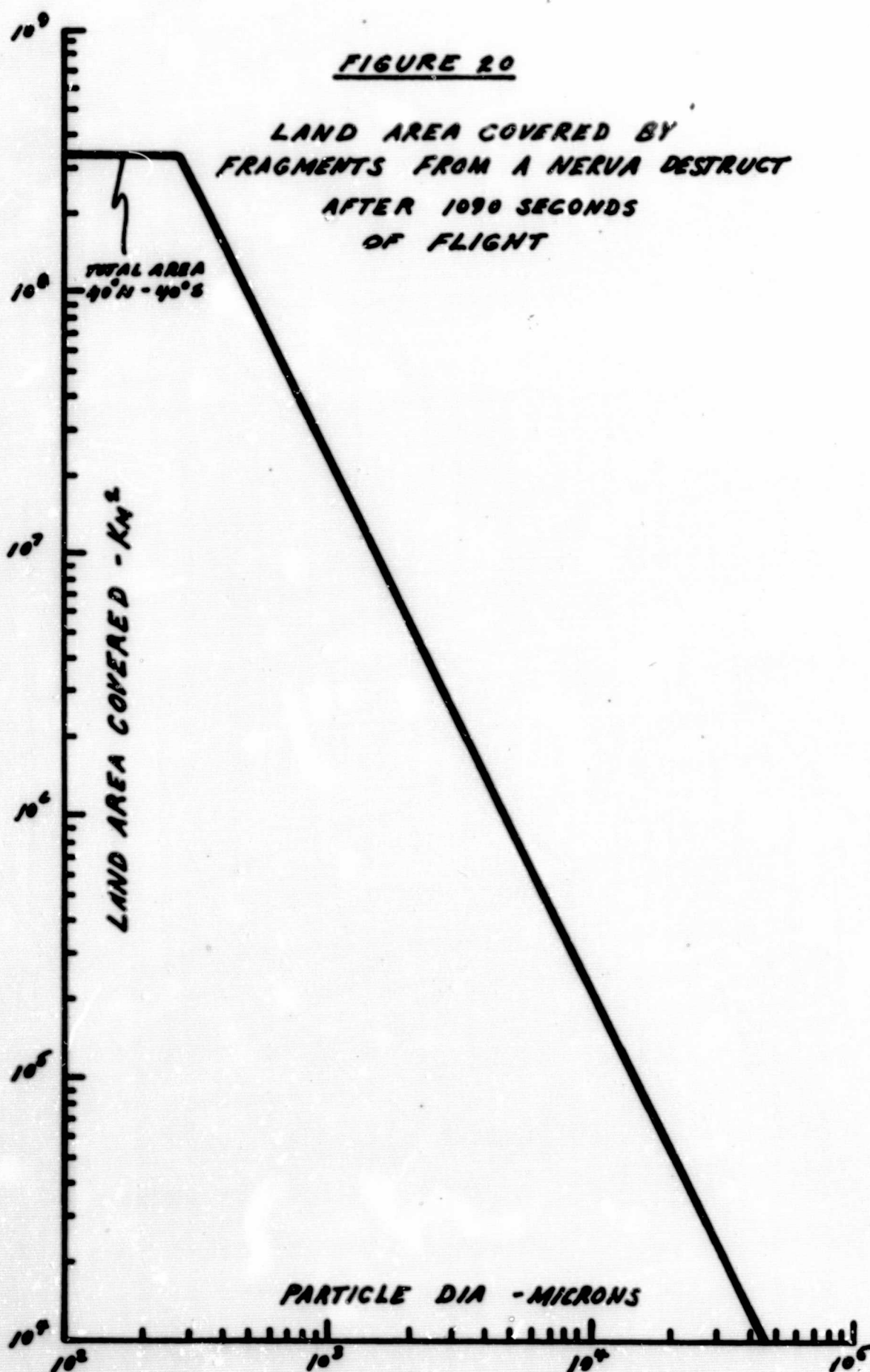
TABLE IV

NUMBER OF PARTICLES AND
EARTH AREA COVERED

Part Dia. (microns)	Area Covered (Km^2)	No. of Particles of Mean Size	
		Nuclear Destruct	Explosive Destruct
3.16	3.3×10^8	3.85×10^{10}	6.0×10^{12}
5.6	"	1.43×10^{10}	1.0×10^{13}
10	"	2.53×10^9	4.4×10^{12}
17.8	"	2.7×10^8	1.2×10^{12}
31.6	"	5.0×10^7	3.2×10^{11}
56.0	"	1.0×10^8	6.4×10^{10}
100	"	1.1×10^8	1.25×10^{10}
178	"	8.4×10^7	2.5×10^9
316	2.5×10^8	1.2×10^7	7.2×10^8
560	7.6×10^7	2.0×10^6	2.1×10^8
1000	2.3×10^7	1.4×10^6	4.1×10^7
1780	7.6×10^6	4.3×10^5	1.4×10^7
3160	2.3×10^6	1.0×10^5	7.2×10^6
5600	7.6×10^5	5.0×10^4	7.6×10^5
10000	2.3×10^5	3.0×10^4	3.7×10^4
17,800	7.6×10^4	1.75×10^4	3.12×10^3
26,900 (explosive)	3.3×10^4	–	35
56,000 (nuclear)	7.3×10^3	4.5×10^3	–
100,000 (nuclear)	2.3×10^3	5.5×10^3	–

TABLE V

AREAL DENSITY OF FRAGMENTS

| Particle Diameter (microns) | Areal Density (particle $/km^2$) | |
	Nuclear Destruct	Explosive Destruct*
3.16	114	1.77×10^4
5.6	42.4	2.96×10^4
10.0	7.5	1.30×10^4
17.8	0.8	3.55×10^3
31.6	0.148	945
56.0	0.296	189
100	0.326	37.0
178	0.248	7.40
316	4.8×10^{-2}	2.90
560	2.6×10^{-2}	2.85
1000	6.1×10^{-2}	1.78
1780	5.65×10^{-2}	1.84
3160	4.35×10^{-2}	3.13
5600	6.59×10^{-2}	1.00
10000	1.30×10^{-1}	1.61×10^{-1}
17,800	2.3×10^{-1}	4.10×10^{-2}
26,900	-	1.06×10^{-3}
56,000	6.15×10^{-1}	-
100,000	2.40	-

* Based on uniform dispersion of particles; actual density may vary from 0.54 to 2.6 times density shown.

throughout the particle volume uniformly; thus, using the weight per particle shown on Figure 2 results in the data shown in Table VI under high explosive destruct.

The nuclear destruct transient would add about 1×10^{21} fissions to the above inventory. However, this contributes less than 10% of the inventory and is, consequently, neglected. The inventory due to operation in the case of nuclear destruct is reduced from 1.75×10^{22} fissions to 5.84×10^{21} because of the amount of fission products vaporized, which in the KIWI-TNT was estimated to be 2/3 of the total inventory.

The inventory in each particle from a nuclear destruct is calculated under the assumption that the fission products are distributed uniformly over the surface of the particle. Thus, using Figure 16 to obtain the number of particles in each size range and assuming spherical particles, the data shown in Table VI for nuclear destruct are obtained.

Table VI data are used in the following sections to obtain the doses for the particular exposure route and the values in Table V are used to obtain the exposure probabilities for the various dose routes. At this point it should be emphasized that the particle fission product inventory does not consider the effects of burnup during re-entry. Burnup would probably remove a significant portion of the fission product inventory from the particles created by nuclear destruct since it appears that most of the remaining fission products condense on the surface of the particle. This effect could reduce or eliminate all exposures following nuclear destruct. Unfortunately, there is no experimental data regarding the inventory reduction that could reasonably be expected. The conclusions in this report are reached assuming that ablation does not affect fission product inventory.

A.   <u>EXTERNAL WHOLE BODY DOSE</u>

Section III-A of this report presented a basis for estimating the population exposure to what might be called an average world population.

The population exposure per unit ground area covered by particles of size j is

$$(P.E.)_j = \phi \left(\frac{\text{man rad}}{\text{fission}} \right) \times \left(\frac{\text{fissions}}{\text{particle}} \right) \frac{\text{particles}}{\text{km}^2}$$

TABLE VI

FISSION INVENTORY

Particle Dia. μ	Fission Inventory (fission/part)	
	Explosive Destruct	Nuclear Destruct
3.14	1.17×10^6	9.2×10^8
5.6	5.85×10^6	2.92×10^9
10.0	3.62×10^7	9.2×10^9
17.8	1.87×10^8	2.92×10^{10}
31.6	1.17×10^9	9.2×10^{10}
56.0	5.85×10^9	2.92×10^{11}
100	3.62×10^{10}	9.2×10^{11}
178	1.87×10^{11}	2.92×10^{12}
316	1.17×10^{12}	9.2×10^{12}
560	5.85×10^{12}	2.92×10^{13}
1000	3.62×10^{13}	9.2×10^{13}
1780	1.87×10^{14}	2.92×10^{14}
3160	9.35×10^{14}	9.2×10^{14}
5600	5.85×10^{15}	2.92×10^{15}
10000	2.58×10^{16}	9.2×10^{15}
17,800	9.35×10^{16}	2.92×10^{16}
26,900	1.87×10^{17}	-
56,000	-	2.92×10^{17}
100,000	-	9.2×10^{17}

If the results are summed for all particle sizes the total population exposure per unit area is obtained. Table VII shows the population exposure per unit area resulting from both explosive and nuclear destruct. The results are given for the center of the "footprint" where all size class particles are presumed to be deposited. As mentioned earlier the results for the case of explosive destruct may vary by a factor of 0.54 to 2.6 as a consequence of the non-uniform dispersion. However, the population exposure resulting from nuclear destruct is, at the least, 50 times greater than that which could occur as a result of explosive destruct due to the smaller number of particles and the consequent higher activity per particle. The area covered by all size class particles is 2.3×10^3 km^2 and, hence, the population dose following nuclear destruct would be

$$192 \text{ man rad/km}^2 \ (2.3 \times 10^3 \text{ km}^2) = 4.4 \times 10^5 \text{ man rad.}$$

The average population density used in the MOREDO model was 25.6 persons/km^2, therefore, the average individual dose from nuclear destruct would be

$$192 \ \frac{\text{man rad}}{\text{km}^2} \ \frac{\text{km}^2}{25.6 \text{ persons}} = 7.5 \text{ rad}$$

while for a explosive destruct the average dose per person would be 0.054 rad.

B. GASTROINTESTINAL EXPOSURE

Figure 18 shows the mean gastrointestinal particle exposure per person per unit particle deposition. This, when multiplied by the deposition density of the particles, yields the mean number of particles per person as shown in Table VIII. These values can also be interpreted as the probability that a person will inhale one particle of that size[3].

Table IX shows the beta dose per particle calculated on the basis that the organ-averaged dose is the total beta decay energy deposited over the entire mass of the organ of interest.* The average beta

---

*This method for dose calculation is used here only for simplicity since more precise calculation methods would be more time consuming and only the relative doses between the two destruct modes are of primary interest here.

TABLE VII

POPULATION EXPOSURE–WHOLE BODY

Particle Dia. μ	Population Exposure (Man-rad/km^2)	
	Explosive Destruct	Nuclear Destruct
3.16	1.47×10^{-6}	8.4×10^{-6}
5.6	1.38×10^{-5}	9.9×10^{-6}
10.0	3.76×10^{-5}	5.5×10^{-6}
17.8	5.30×10^{-5}	1.87×10^{-6}
31.6	8.85×10^{-5}	1.09×10^{-6}
56.0	8.81×10^{-5}	6.95×10^{-6}
100	1.07×10^{-4}	2.39×10^{-5}
178	1.11×10^{-4}	5.8×10^{-5}
316	2.71×10^{-4}	3.53×10^{-5}
560	1.33×10^{-3}	6.06×10^{-5}
1000	5.15×10^{-3}	4.44×10^{-4}
1780	2.75×10^{-2}	1.33×10^{-3}
3160	2.34×10^{-1}	3.19×10^{-3}
5600	4.68×10^{-1}	1.53×10^{-2}
10000	3.33×10^{-1}	9.56×10^{-2}
17,800	3.06×10^{-1}	5.4×10^{-1}
26,900	1.58×10^{-2}	-
56,000	-	14.4
100,000	-	177
Total	~1.39 Man rad/km^2	~192 Man rad/km^2

TABLE VIII

G. I. EXPOSURE VIA INHALATION

Particle Dia.	Mean Exposure $\psi_S/\frac{-}{m}\left(\frac{km^2}{person}\right)$	Mean Exposure $\psi_S \left(\frac{part}{person}\right)$	
		Explosive Destruct	Nuclear Destruct
3.16	1.5×10^{-6}	2.66×10^{-2}	1.71×10^{-4}
5.6	3.2×10^{-7}	9.47×10^{-3}	1.35×10^{-5}
10.0	1×10^{-7}	1.30×10^{-3}	7.50×10^{-7}
17.8	3.4×10^{-8}	1.21×10^{-4}	2.72×10^{-8}
31.6	1.3×10^{-8}	1.23×10^{-5}	1.92×10^{-9}
56.0	5.0×10^{-9}	9.45×10^{-7}	1.48×10^{-9}
100	2.0×10^{-9}	7.40×10^{-8}	6.52×10^{-10}
178	8.6×10^{-10}	6.35×10^{-9}	2.14×10^{-10}
316	4.2×10^{-10}	1.22×10^{-9}	2.02×10^{-11}
560	2.3×10^{-10}	6.55×10^{-10}	5.97×10^{-11}
1000	1.4×10^{-10}	2.49×10^{-10}	8.55×10^{-11}

TABLE IX

AVERAGE ORGAN (lower large intestine) DOSE

Particle Dia. microns	High Explosive Destruct (rads)	Nuclear Destruct (rads)
3.14	2.24×10^{-2}	1.98×10^{1}
5.60	1.13×10^{-1}	6.31×10^{1}
10.0	7.0×10^{-1}	1.98×10^{2}
17.8	3.62×10^{-1}	6.31×10^{2}
31.6	2.26×10^{1}	1.98×10^{3}
5610	1.13×10^{2}	6.31×10^{3}
100	7.00×10^{2}	1.98×10^{4}
178	3.42×10^{3}	5.95×10^{4}
316	1.90×10^{4}	1.67×10^{5}
560	7.70×10^{4}	4.3×10^{5}
1000	2.42×10^{5}	1.05×10^{6}

energy between 1 and 30 hours following fission is about 1.5 Mev. Since the material reenters relatively quickly and since G.I. exposure will last, on the average, about 30 hours[3] this represents a reasonable beta energy for the exposure interval.

The data from Tables VIII and IX can be combined to yield curves of the probability of receiving a given dose from a single particle as shown in Figure 21. It can be seen that the curves for nuclear and explosive destruct approach one another for high dose-low probability interactions and consequently there is little choice as to the more advantageous destruct system on this basis. However, for interactions of reasonably high probabilities--with lower dose values, it can be seen that the explosive destruct system would result in dose values which are lower by a factor of one-fifth. The area to which Figure 21 applies is-

$$2.3 \times 10^3 \text{ km}^2 \text{ containing } \frac{25.6 \text{ people}}{\text{km}^2} \text{ or } 56,000 \text{ people.}$$

Thus, it can be seen that the expected number of people who may receive significant doses from this route as a result of a nuclear destruct is not negligible. Consequently, it must be concluded that from the standpoint of exposure of the lower large intestine the high explosive destruct system would present a preferable exposure situation.

C. LUNG EXPOSURE

For the smallest class of particle considered i.e., 3.1 microns, the probability of exposure of one person to one particle and the dose per particle (organ averaged dose) is given in Table X.

The upper limit of particle size that will reach the lung is on the order of 15 μ. As can be seen from Table X the probability for a particle of the indicated size to be inhaled and reach the lung is greater for debris generated by explosive destruct while the dose delivered per particle is higher following nuclear destruct. The largest expected number of people who will inhale one particle which reaches the lung occurs with the explosive destruct mode; 62 are exposed in this case. For nuclear destruct,

FIGURE 21

DOSE PER PARTICLE VS PROBABILITY OF INGESTING (VIA INHALATION) OF A SINGLE PARTICLE

-51-
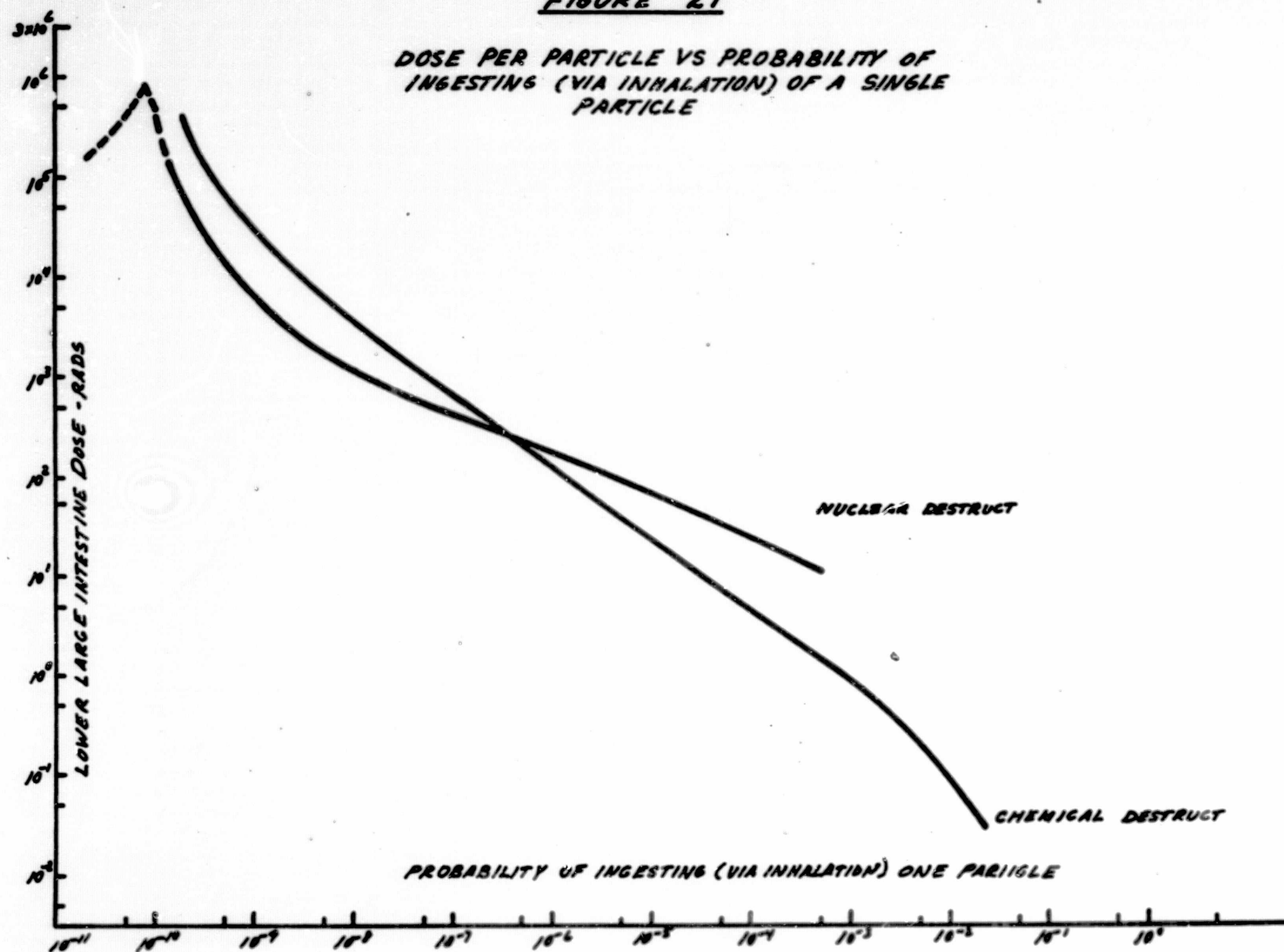
less than one person would be expected to be exposed. Table X indicates that no definite conclusion can be drawn as to the destruct system which offers the greater degree of safety since the high doses are associated with reasonably small probabilities and the dose values are not excessively high.

D.   SKIN EXPOSURE

Figure 19 shows how the mean skin exposure per person per particle per unit area varies with particle size. Although no upper size limit has been established by direct experimentation this size is probably about 1000 microns (1mm) in diameter. Above this size, the particle would probably be noticed by the individual and be removed. Hence, for this report 1000 microns is assumed to be the upper limit.

Table XI gives the mean number of particles per person expected to impact and stick to a persons' skin and the dose rate expected from a single particle. The results indicate that for skin contact exposure, the   explosive destruct system will result in a greater probability of exposure because of the greater number of particles formed but will result in a lower dose rate for a given size particle compared to a particle from a nuclear destruct.

TABLE X

LUNG EXPOSURE

| | Mean Exposure, particles/person | | Dose Rate (at one hour after shutdown) Rad/day | |
Particle Dia.	Nuclear Destruct	High Explosive Destruct	Nuclear Destruct	High Explosive Destruct
3.16	7.13×10^{-6}	1.11×10^{-3}	0.655	8.4×10^{-4}
14.1	1.78×10^{-9}	3.56×10^{-6}	14.3	9.4×10^{-2}

TABLE XI

SKIN CONTACT EXPOSURE FROBABILITY

Particle Dia. (microns)	Mean No. Particles Per Person*		Dose rate rad/hr/particle	
	Nuclear Destruct	Explosive Destruct	Nuclear Destruct	Explosive Destruct
3.14	1.31×10^{-5}	2.04×10^{-3}	1.53×10^{-5}	1.94×10^{-8}
5.60	1.69×10^{-5}	1.18×10^{-2}	4.86×10^{-5}	9.70×10^{-8}
10.0	7.12×10^{-6}	1.23×10^{-2}	1.53×10^{-4}	6.00×10^{-7}
17.8	1.2×10^{-6}	5.31×10^{-3}	4.86×10^{-4}	3.10×10^{-6}
31.6	1.85×10^{-7}	1.18×10^{-3}	1.53×10^{-3}	1.94×10^{-5}
56.0	2.01×10^{-7}	1.28×10^{-4}	4.86×10^{-3}	9.70×10^{-5}
100	1.24×10^{-7}	1.41×10^{-5}	1.53×10^{-2}	6.00×10^{-4}
178	5.70×10^{-8}	1.70×10^{-6}	4.46×10^{-2}	2.86×10^{-3}
316	6.95×10^{-9}	4.20×10^{-7}	1.25×10^{-1}	1.59×10^{-2}
560	2.60×10^{-9}	2.85×10^{-7}	3.4×10^{-1}	6.70×10^{-2}
1000	5.00×10^{-9}	1.46×10^{-7}	8.1×10^{-1}	3.18×10^{-1}

*Or probability of one person being exposed to one particle of given size.

V. CONCLUSIONS

From the material presented in this report two major sets of con-
clusions may be reached. The first set of conclusions are con-
cerned with the comparison of the radiological consequences of a
nuclear or high explosive destruct and are based upon the avail-
able experimental results of high explosive tests and the KIWI-TNT
test. The second set of conclusions concerns the experimental
data itself.

Based on experimental data and the dose and interaction models
developed for the safety analysis program of the ROVER project,
a comparison of the radiological consequences of nuclear and
high explosive destruct reveals that for a destruct after about
1100 seconds which will cause impact of the particles on the
South African continent:

> (1)   A nuclear destruct will result in an external whole
> body gamma dose of no greater than 7.5 rads when averaged
> over the entire population group. For the same case the
> chemical explosive destruct system will cause a dose of
> only 0.03 rads to 0.14 rads depending upon the orientation
> of the vehicle at the time of destruct. (Individual doses can
> be considerably higher in both cases.)

> (2)   The nuclear destruct system results in a higher dose
> to the lower large intestine for a given probability than the
> explosive destruct system. For the nuclear destruct system
> one person may be expected to receive a dose to the LLI on
> the order of 73 rads whereas the explosive destruct system
> would result in a dose of about 25 rads.

> (3)   For important probabilities of exposure neither the
> explosive nor the nuclear destruct system results in signif-
> icant doses to the lung; however, explosive destruct results
> in a greater probability of exposure but a lower dose rate for
> the same size particle.

(4)   Neither destruct system appears to deliver significant skin contact dose with important exposure probabilities; however, the explosive destruct system results in a greater exposure probability but a lower dose for any given size particle.

(5)   The degree of fission product removal by ablation during re-entry is unknown and has not been considered in the comparison. Significant ablation effects, especially for particles generated from a nuclear destruct can significantly affect conclusions 1 to 4 above.

The following conclusions apply to the experimental data:

(1)   Operating and post operational temperature effects significantly alter the particle size and uranium distribution of the resulting debris from either destruct system.

(2)   Actual geometry of the high explosive projectiles in a flight configuration destruct system might significantly alter size distribution and ground deposition of debris.

(3)   Timing of the high explosive detonation might affect size distribution and ground deposition of debris.

(4)   The method of initiating a nuclear destruct transient might significantly alter size distribution and ground deposition of debris.

(5)   The high explosive destruct tests conducted to date do not adequately reproduce conditions that exist at the time of destruct with a flight configuration system. Therefore, the consequences to a population affected by the debris generated can not be predicted with a high degree of confidence.

(6)   The KIWI-TNT experiment, which was not a nuclear destruct demonstration, provides some insight as to the capabilities of a nuclear destruct but does not provide the data required to predict consequences to populations with a reasonable degree of confidence.

VI. RECOMMENDATIONS

1.   Future explosive destruct tests should simulate as much as possible an actual flight configuration destruct system.

2.   Future explosive destruct tests should simulate a reactor core which has been operating for some specified interval and should simulate the temperature conditions which could exist at the time of destruct.

3.   Plasma jet studies should be undertaken to determine the degree of fission product ablation which can occur with particles generated by a nuclear destruct.

VII. REFERENCES

1. "ROVER Flight Safety Program Preliminary Review - Volume II
    Safety Analysis Report - Evaluation of Passive Re-Entry Approach",
    Westinghouse Astronuclear Laboratory, C-RD (Sept. 30, 1965).

2. "ROVER Flight Safety Program Preliminary Review - Volume I
    Safety Analysis Report - Evaluation of Destruct and Auxiliary
    Thrust Systems", Lockheed Missiles and Space Co., and
    Marshall Space Flight Center, C-RD (Sept. 30, 1965).

3. De Agazio, Albert W., "Dose Calculation Models for Re-Enter-
    ing Nuclear Rocket Debris", NUS-229 (Rev.) NUS Corp. (Oct.
    1965).

4. "ROVER Flight Safety Program Preliminary Review - Volume IV -
    Radiological Considerations in Nuclear Flight Safety", SNPO
    Radiological Effects Working Groups, (To be published).

5. "ROVER Flight Safety Program Preliminary Review - Volume III
    Part B - Post Operational Destruct System", Picatinny Arsenal,
    C-RD (December 1965).

6. Rinder, R. M., "Establishment of Safety Criteria for use in
    Engineering of Explosive Facilities and Operation, Report #2.
    Detonation by Fragment Impact", NP 11435, Aberdeen Proving
    Grounds, (September 1961).

7. Dutschke, W., "Engineer Design Test of NERVA Countermeasures",
    DPS-1876, Aberdeen Proving Grounds, (February 1966).

8. Campbell, E. E., Moss, W. D., "Particle Size Distribution
    from a One-Ninth Scale ROVER Reactor Axial - H. E. Destruct",
    LA-3214-MS Los Alamos Scientific Laboratory (December 15,
    1964).

9. NERVA Destruct System Status Meeting, Lewis Research Center,
    February 10, 1966.

10. Personal Communication, A. J. Clark, Sandia Corp. to M. I.
    Goldman, NUS Corp., December 1, 1965.

11. Personal Communication L.D.P. King and E.E. Campbell, Los Alamos Scientific Laboratory.

12. "Quarterly Status Report of LASL ROVER Program for Period Ending February 28, 1965, LA-3280-MS, Los Alamos Scientific Laboratory.

13. King, L.D.P., Mills, C.B., "Some Feasibility Studies of the Nuclear Destruct Concept for ROVER Reactor Disposal", Presented at 1965 Winter Meeting American Nuclear Society at Washington, D.C.

14. Personal Communication with E. Freiling and J. Lai, United States Naval Radiological Defense Laboratory.

15. Kim, Y.S., MOREDO , NUS Mobile Receptor Dose Program, NUS-257, NUS Corporation, (October 12, 1965).

16. Garcia, L.F., Sitton, J.F., "Age/Occupation and $(f,2,\sigma)$ Values for Sets of NUS-230 Based on 1962 Population Data", Unpublished Addenda to NUS-230, May 21, 1965, S-RD.

17. Perkins, J.F., and King, R.W., "Energy Release from the Decay of Fission Products", <u>Nuclear Science and Engineering</u>, Vol. 3, 726 (1958).

18. Radd, H., "Nuclear Vehicle Flight Safety Study Summary Report for Phases 1 and 2, LMSC-B061396, Lockheed Missiles and Space Company, July 31, 1963.